

# Klimaänderung II

## 7. Der Energiehaushalt der Erde, Klima-Rückkopplungen und Klima-Sensitivität

Robert Sausen

Institut für Physik der Atmosphäre  
Deutsches Zentrum für Luft- und Raumfahrt  
Oberpfaffenhofen

Vorlesung SS 2022

LMU München



Knowledge for Tomorrow

# Klausur

- **Theresienstr. 39, B 040**
- **20.07.2023, 14:15**
- **Dauer: 2 h**

Hilfsmittel: Kugelschreiber (blau oder schwarz)  
1 A4-Blatt, handgeschrieben (eigene Handschrift)  
einfacher Taschenrechner (kein Smartphone)



## Technical information

- <http://www.pa.op.dlr.de/~RobertSausen/vorlesung/index.html>
  - Most recent update on the lecture
  - Slides of the lecture (with some delay)
  
  - See also LSF <https://lsf.verwaltung.uni-muenchen.de/>
  
- Contact: robert.sausen@dlr.de
  
- Further information:
  - [www.ipcc.ch](http://www.ipcc.ch)
  - [www.de-ipcc.de](http://www.de-ipcc.de)



# Contents of IPCC AR 6 2021

## Working Group I: the Physical Science Basis

Chapters	
Chapter 1: Framing, context, methods	DOWNLOAD
Chapter 2: Changing state of the climate system	DOWNLOAD
Chapter 3: Human influence on the climate system	DOWNLOAD
Chapter 4: Future global climate: scenario-based projections and near-term information	DOWNLOAD
Chapter 5: Global carbon and other biogeochemical cycles and feedbacks	DOWNLOAD
Chapter 6: Short-lived climate forcers	DOWNLOAD
Chapter 7: The Earth's energy budget, climate feedbacks, and climate sensitivity	DOWNLOAD
Chapter 8: Water cycle changes	DOWNLOAD
Chapter 9: Ocean, cryosphere, and sea level change	DOWNLOAD
Chapter 10: Linking global to regional climate change	DOWNLOAD
Chapter 11: Weather and climate extreme events in a changing climate	DOWNLOAD
Chapter 12: Climate change information for regional impact and for risk assessment	DOWNLOAD
Atlas	DOWNLOAD
Supplementary Material	▼
Annexes	▼

<https://www.ipcc.ch/report/ar6/wg1/#FullReport>



# Chapter 7: Short-lived Climate Forcers

## Coordinating Lead Authors:

Piers Forster (United Kingdom), Trude Storelvmo (Norway)

## Lead Authors:

Kyle Armour (United States of America), William Collins (United Kingdom), Jean-Louis Dufresne (France), David Frame (New Zealand), Daniel J. Lunt (United Kingdom), Thorsten Mauritsen (Sweden/Denmark), Matthew D. Palmer (United Kingdom), Masahiro Watanabe (Japan), Martin Wild (Switzerland), Hua Zhang (China)



# Chapter 7: Short-lived Climate Forcers

## Contributing Authors:

Kari Alterskjær (Norway), Chris Smith (United Kingdom), Govindasamy Bala (India/United States of America), Nicolas Bellouin (United Kingdom/France), Terje Berntsen (Norway), Fábio Boeira Dias (Finland/Brazil), Sandrine Bony (France), Natalie J. Burls (United States of America/South Africa), Michelle Cain (United Kingdom), Catia M. Domingues (Australia, United Kingdom/Brazil), Aaron Donohoe (United States of America), Mark Flanner (United States of America), Jan S. Fuglestad (Norway), Lily C. Hahn (United States of America), Glen R. Harris (United Kingdom/New Zealand, United Kingdom), Christopher Jones (United Kingdom), Seiji Kato (United States of America), Jared Lewis (Australia/New Zealand), Zhanqing Li (United States of America), Mike Lockwood (United Kingdom), Norman Loeb (United States of America), **Jochem Marotzke (Germany)**, **Malte Meinshausen (Australia/Germany)**, **Sebastian Milinski (Germany)**, Zebedee R.J. Nicholls (Australia), Ryan S. Padron Flasher (Switzerland/Ecuador, United States of America), **Anna Possner (Germany)**, Cristian Proistosescu (Romania), **Johannes Quaas (Germany)**, Joeri Rogelj (United Kingdom/Belgium), Daniel Rosenfeld (Israel), Bjørn H. Samset (Norway), Abhishek Savita (Australia/India), Jessica Vial (France), **Karina von Schuckmann (France/Germany)**, Mark Zelinka (United States of America), Shuyun Zhao (China)



# Chapter 7: Short-lived Climate Forcers

## Review Editors:

Robert Colman (Australia), H. Damon Matthews (Canada), Venkatachalam Ramaswamy (United States of America)

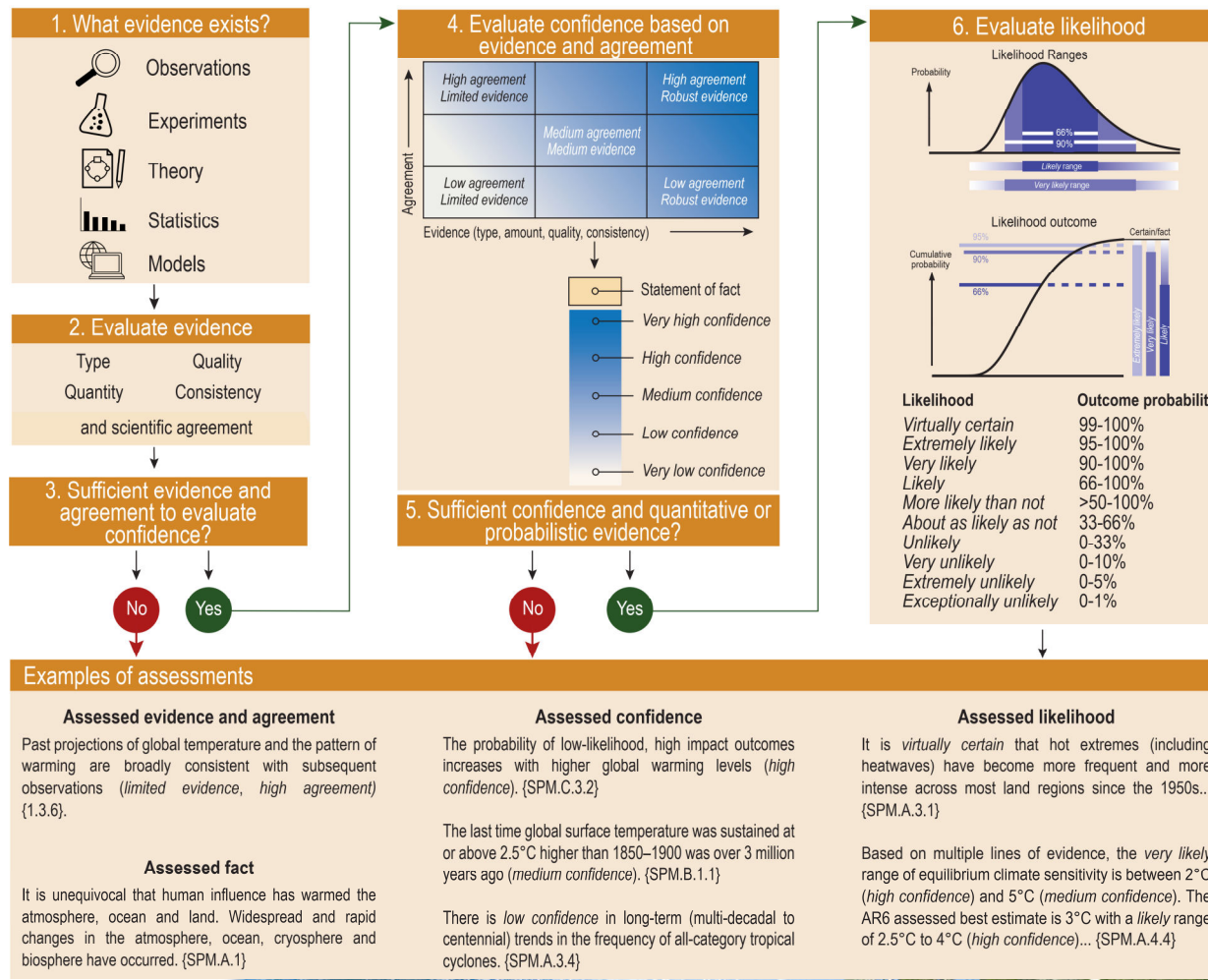
## Chapter Scientists:

Kari Alterskjær (Norway), Chris Smith (United Kingdom)

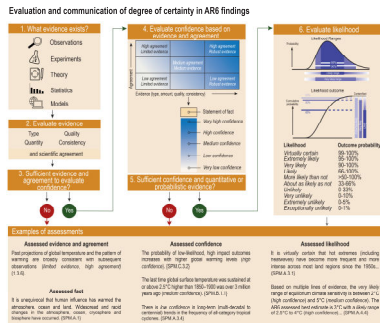




## Evaluation and communication of degree of certainty in AR6 findings







### 4. Evaluate confidence based on evidence and agreement

Agreement ↑	High agreement Limited evidence		High agreement Robust evidence
		Medium agreement Medium evidence	
	Low agreement Limited evidence		Low agreement Robust evidence

Evidence (type, amount, quality, consistency) →

### 5. Sufficient confidence and quantitative or probabilistic evidence?

↓ No (Red circle)      ↓ Yes (Green circle)

- Statement of fact
- Very high confidence
- High confidence
- Medium confidence
- Low confidence
- Very low confidence

### 6. Evaluate likelihood

**Likelihood Ranges**

Probability

66%  
90%

Likely range  
Very likely range

**Likelihood outcome**

Cumulative probability

95%  
90%  
66%

Certain/fact

Extremely likely  
Very likely  
Likely

Likelihood	Outcome probability
Virtually certain	99-100%
Extremely likely	95-100%
Very likely	90-100%
Likely	66-100%
More likely than not	>50-100%
About as likely as not	33-66%
Unlikely	0-33%
Very unlikely	0-10%
Extremely unlikely	0-5%
Exceptionally unlikely	0-1%

## Chapter 7: The Earth's energy budget

Chapter 7 assesses the major physical processes affecting the evolution of Earth's energy budget and the associated changes in temperature and the climate system.

**Section 7.1**  
Introduction and advances

**Section 7.2**  
Energy budget

**Section 7.3**  
Radiative forcing

**Section 7.4**  
Climate feedbacks

**Section 7.5**  
Climate sensitivity

**Section 7.6**  
Metrics

**FAQs**

## Chapter 7: Quick guide

Key topics and corresponding sub-sections

- Aerosols  
7.3.3 | 7.3.5 | FAQ 7.2
- Clouds  
7.3.3.2 | 7.4.2.4 | FAQ 7.2
- Emission metrics and climate policy  
7.6.2
- Observations of Earth's energy budget  
7.2 | FAQ 7.1
- Paleoclimate data  
7.4.3.2 | 7.5.3
- Polar amplification  
7.4.4.1
- Synthesis of forcing, feedbacks and climate sensitivity  
7.3.5 | 7.4.2.7 | 7.5.5 | FAQ 7.3

### Boxes

**Box 7.1**  
Energy budget framework

**Box 7.2**  
Global energy budget

**Box 7.2**  
Physical considerations in emission-metric choice

### Cross-chapter boxes

**CC Box 7.1**  
Physical emulation of Earth system models



## Statements in the Executive Summary (1)

This chapter assesses the present state of knowledge of Earth's energy budget: that is, the main flows of energy into and out of the Earth system, and how these energy flows govern the climate response to a radiative forcing. Changes in atmospheric composition and land use, like those caused by anthropogenic greenhouse gas emissions and emissions of aerosols and their precursors, affect climate through perturbations to Earth's top-of-atmosphere energy budget.



## Statements in the Executive Summary (1)

This chapter assesses the present state of knowledge of Earth's energy budget: that is, the main flows of energy into and out of the Earth system, and how these energy flows govern the climate response to a radiative forcing. Changes in atmospheric composition and land use, like those caused by anthropogenic greenhouse gas emissions and emissions of aerosols and their precursors, affect climate through perturbations to Earth's top-of-atmosphere energy budget. The effective radiative forcings (ERFs) quantify these perturbations, including any consequent adjustment to the climate system (but excluding surface temperature response). How the climate system responds to a given forcing is determined by climate feedbacks associated with physical, biogeophysical and biogeochemical processes. These feedback processes are assessed, as are useful measures of global climate response, namely equilibrium climate sensitivity (ECS) and the transient climate response (TCR).



## Statements in the Executive Summary (1)

This chapter assesses the present state of knowledge of Earth's energy budget: that is, the main flows of energy into and out of the Earth system, and how these energy flows govern the climate response to a radiative forcing. Changes in atmospheric composition and land use, like those caused by anthropogenic greenhouse gas emissions and emissions of aerosols and their precursors, affect climate through perturbations to Earth's top-of-atmosphere energy budget. The effective radiative forcings (ERFs) quantify these perturbations, including any consequent adjustment to the climate system (but excluding surface temperature response). How the climate system responds to a given forcing is determined by climate feedbacks associated with physical, biogeophysical and biogeochemical processes. These feedback processes are assessed, as are useful measures of global climate response, namely equilibrium climate sensitivity (ECS) and the transient climate response (TCR). This chapter also assesses emissions metrics, which are used to quantify how the climate response to the emissions of different greenhouse gases compares to the response to the emissions of carbon dioxide (CO<sub>2</sub>).



## Statements in the Executive Summary (1)

This chapter assesses the present state of knowledge of Earth's energy budget: that is, the main flows of energy into and out of the Earth system, and how these energy flows govern the climate response to a radiative forcing. Changes in atmospheric composition and land use, like those caused by anthropogenic greenhouse gas emissions and emissions of aerosols and their precursors, affect climate through perturbations to Earth's top-of-atmosphere energy budget. The effective radiative forcings (ERFs) quantify these perturbations, including any consequent adjustment to the climate system (but excluding surface temperature response). How the climate system responds to a given forcing is determined by climate feedbacks associated with physical, biogeophysical and biogeochemical processes. These feedback processes are assessed, as are useful measures of global climate response, namely equilibrium climate sensitivity (ECS) and the transient climate response (TCR). This chapter also assesses emissions metrics, which are used to quantify how the climate response to the emissions of different greenhouse gases compares to the response to the emissions of carbon dioxide (CO<sub>2</sub>). This chapter builds on the assessment of carbon cycle and aerosol processes from Chapters 5 and 6, respectively, to quantify non-CO<sub>2</sub> biogeochemical feedbacks and the ERF for aerosols. Other chapters in this Report use this chapter's assessment of ERF, ECS and TCR to help understand historical and future temperature changes (Chapters 3 and 4, respectively), the response to cumulative emissions and the remaining carbon budget (Chapter 5), emissions-based radiative forcing (Chapter 6) and sea level rise (Chapter 9). ...



## Statements in the Executive Summary (1)

This chapter assesses the present state of knowledge of Earth's energy budget: that is, the main flows of energy into and out of the Earth system, and how these energy flows govern the climate response to a radiative forcing. Changes in atmospheric composition and land use, like those caused by anthropogenic greenhouse gas emissions and emissions of aerosols and their precursors, affect climate through perturbations to Earth's top-of-atmosphere energy budget. The effective radiative forcings (ERFs) quantify these perturbations, including any consequent adjustment to the climate system (but excluding surface temperature response). How the climate system responds to a given forcing is determined by climate feedbacks associated with physical, biogeophysical and biogeochemical processes. These feedback processes are assessed, as are useful measures of global climate response, namely equilibrium climate sensitivity (ECS) and the transient climate response (TCR). This chapter also assesses emissions metrics, which are used to quantify how the climate response to the emissions of different greenhouse gases compares to the response to the emissions of carbon dioxide (CO<sub>2</sub>). This chapter builds on the assessment of carbon cycle and aerosol processes from Chapters 5 and 6, respectively, to quantify non-CO<sub>2</sub> biogeochemical feedbacks and the ERF for aerosols. Other chapters in this Report use this chapter's assessment of ERF, ECS and TCR to help understand historical and future temperature changes (Chapters 3 and 4, respectively), the response to cumulative emissions and the remaining carbon budget (Chapter 5), emissions-based radiative forcing (Chapter 6) and sea level rise (Chapter 9). ...



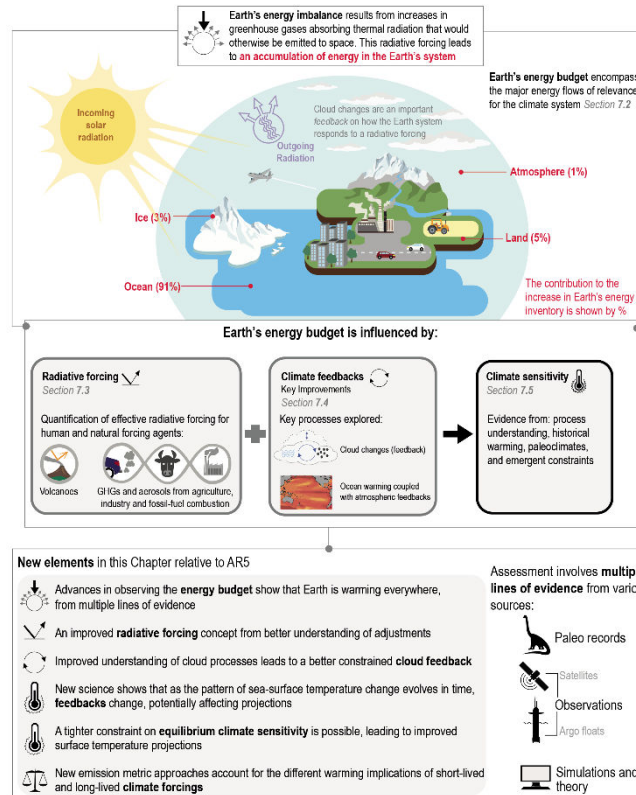
## Statements in the Executive Summary (2)

... This chapter builds on findings from the IPCC Fifth Assessment Report (AR5), the Special Report on Global Warming of 1.5 °C (SR1.5), the Special Report on the Ocean and Cryosphere in a Changing Climate (SROCC) and the Special Report on climate change, desertification, land degradation, sustainable land management, food security, and greenhouse gas fluxes in terrestrial ecosystems (SRCCL). Very likely ranges are presented unless otherwise indicated.



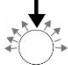


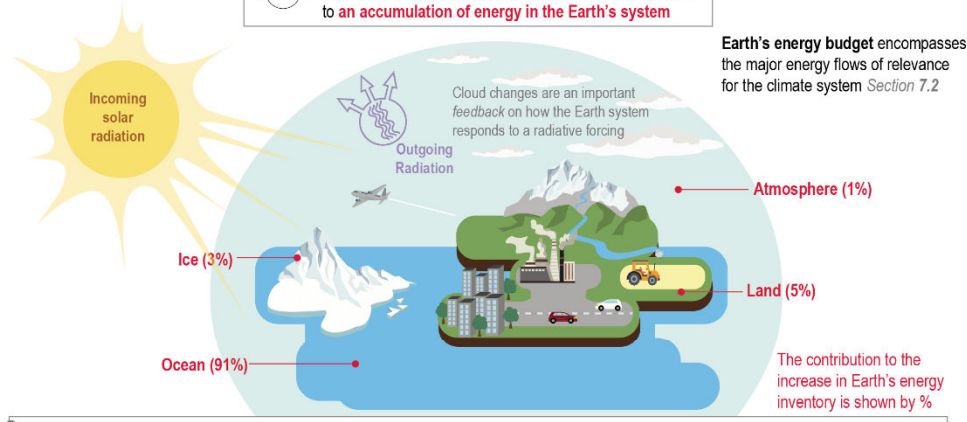
# Visual abstract of the chapter, illustrating why the Earth's energy budget matters and how it relates to the underlying chapter assessment



**Figure 7.1 (continued):** Panel (b) Visual abstract of the chapter, illustrating why the Earth's energy budget matters and how it relates to the underlying chapter assessment. The methods used to assess processes and key new findings relative to AR5 are highlighted. Upper schematic adapted from Von Schuckmann et al. (2020).

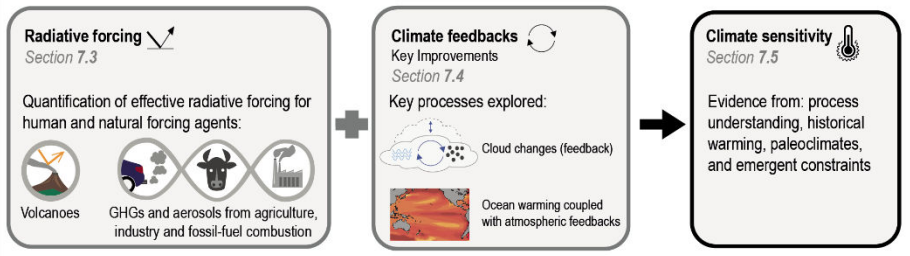


↓  

**Earth's energy imbalance** results from increases in greenhouse gases absorbing thermal radiation that would otherwise be emitted to space. This radiative forcing leads to **an accumulation of energy in the Earth's system**









**Earth's energy budget** encompasses the major energy flows of relevance for the climate system *Section 7.2*






**Earth's energy budget is influenced by:**



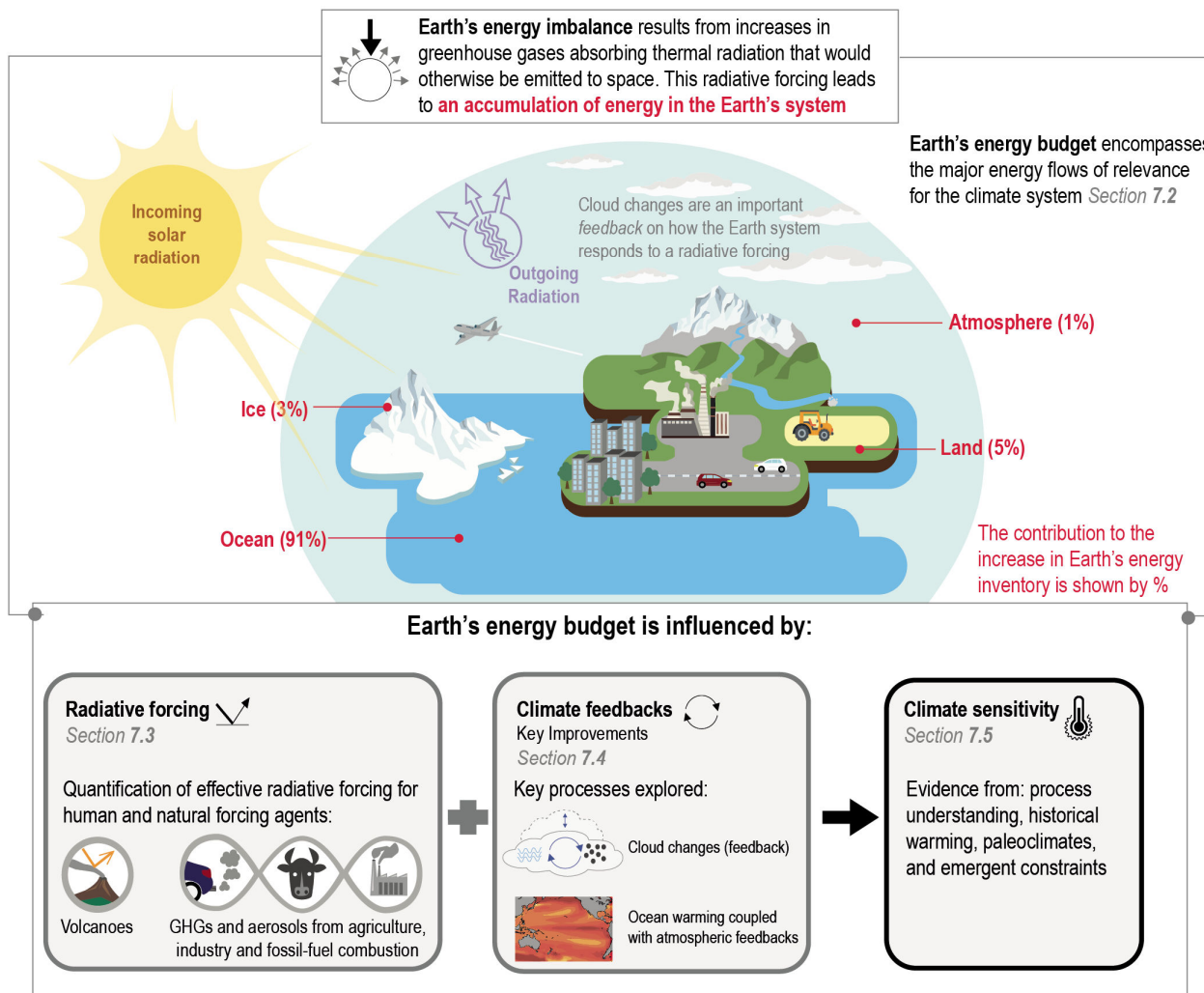
**New elements** in this Chapter relative to AR5

-  Advances in observing the **energy budget** show that Earth is warming everywhere, from multiple lines of evidence
-  An improved **radiative forcing** concept from better understanding of adjustments
-  Improved understanding of cloud processes leads to a better constrained **cloud feedback**
-  New science shows that as the pattern of sea-surface temperature change evolves in time, **feedbacks** change, potentially affecting projections
-  A tighter constraint on **equilibrium climate sensitivity** is possible, leading to improved surface temperature projections
-  New emission metric approaches account for the different warming implications of short-lived and long-lived **climate forcings**

Assessment involves **multiple lines of evidence** from various sources:

-  Paleo records
-  Satellites
-  Observations
-  Argo floats
-  Simulations and theory





05.07.2023

**New elements in this Chapter relative to AR5**

- Advances in observing the **energy budget** show that Earth is warming everywhere, from multiple lines of evidence
- An improved **radiative forcing** concept from better understanding of adjustments
- Improved understanding of cloud processes leads to a better constrained **cloud feedback**
- New science shows that as the pattern of sea-surface temperature change evolves in time, **feedbacks** change, potentially affecting projections
- A tighter constraint on **equilibrium climate sensitivity** is possible, leading to improved surface temperature projections
- New emission metric approaches account for the different warming implications of short-lived and long-lived **climate forcings**

Assessment involves **multiple lines of evidence** from various sources:

- Paleo records
- Satellites
- Observations
- Argo floats
- Simulations and theory

## Statements in the Executive Summary

### *Earth's Energy Budget(1)*

Since AR5, the accumulation of energy in the Earth system, quantified by changes in the global energy inventory for all components of the climate system, has become established as a robust measure of the rate of global climate change on interannual-to-decadal time scales. Compared to changes in global surface air temperature (GSAT), the global energy inventory exhibits less variability, which can mask underlying climate trends. Compared to AR5, there is increased confidence in the quantification of changes in the global energy inventory due to improved observational records and closure of the sea level budget. Energy will continue to accumulate in the Earth system until at least the end of the 21st century, even under strong mitigation scenarios, and will primarily be observed through ocean warming and associated with continued sea level rise through thermal expansion (*high confidence*). {7.2.2, Box 7.2, Table 7.1, Cross-Chapter Box 9.1, Table 9.5, 9.2.2, 9.6.3}



## Schematic representation of the global mean energy budget of the Earth (upper panel), and its equivalent without considerations of cloud effects (lower panel)

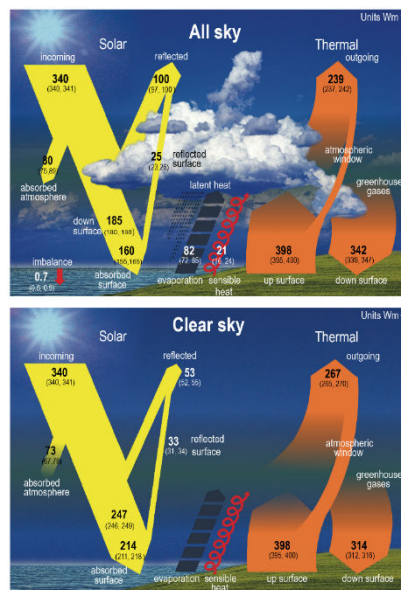
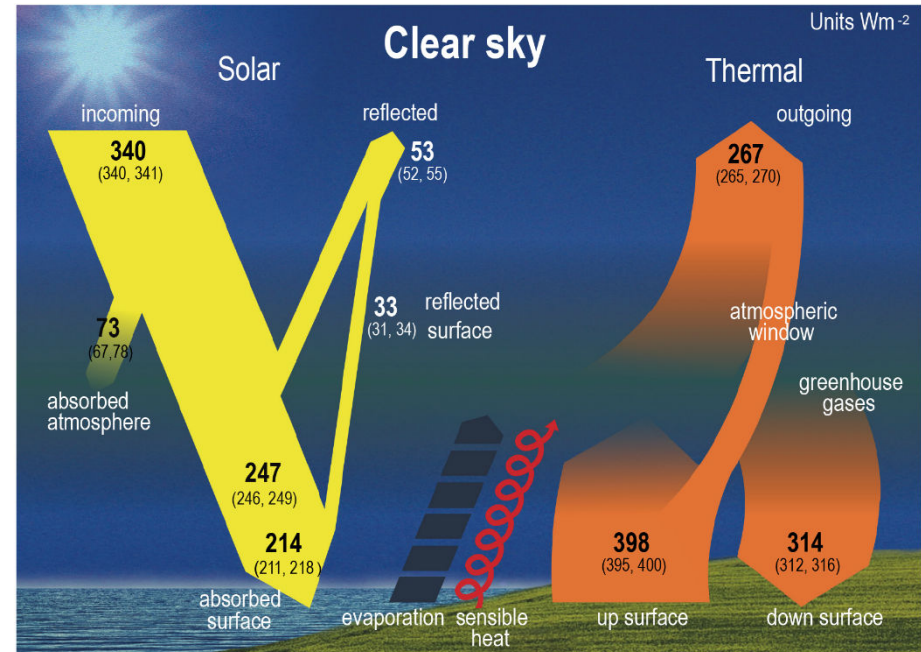
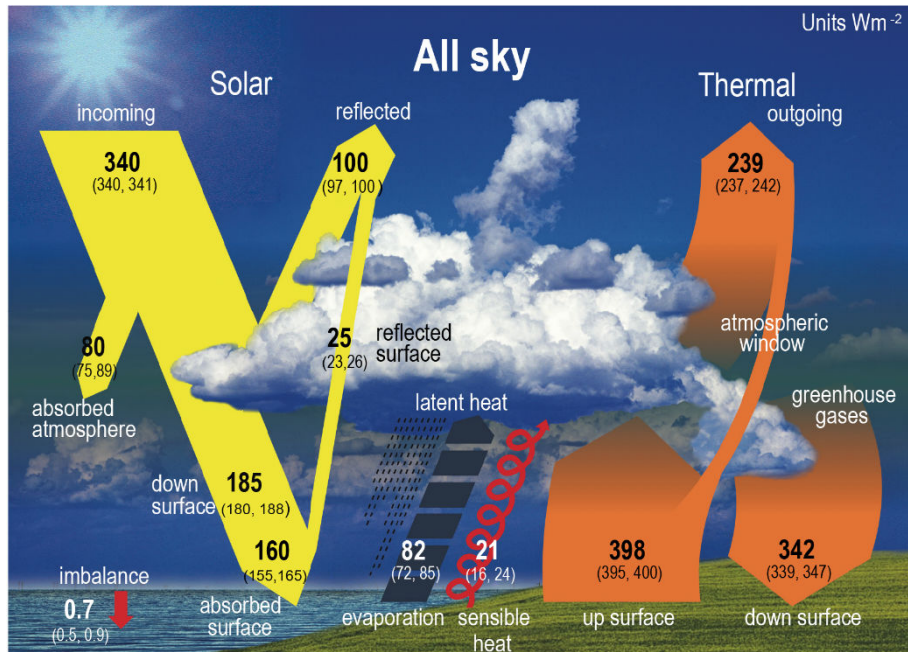


**Figure 7.2 | Schematic representation of the global mean energy budget of the Earth (upper panel), and its equivalent without considerations of cloud effects (lower panel).** Numbers indicate best estimates for the magnitudes of the globally averaged energy balance components in  $W\ m^{-2}$  together with their uncertainty ranges in parentheses (5–95% confidence range), representing climate conditions at the beginning of the 21st century. Note that the cloud-free energy budget shown in the lower panel is not the one that Earth would achieve in equilibrium when no clouds could form. It rather represents the global mean fluxes as determined solely by removing the clouds but otherwise retaining the entire atmospheric structure. This enables the quantification of the effects of clouds on the Earth energy budget and corresponds to the way clear-sky fluxes are calculated in climate models. Thus, the cloud-free energy budget is not closed and therefore the sensible and latent heat fluxes are not quantified in the lower panel. Figure adapted from Wild et al. (2015, 2019).

# Schematic representation of the global mean energy budget of the Earth (upper panel), and its equivalent without considerations of cloud effects (lower panel)



# Statements in the Executive Summary

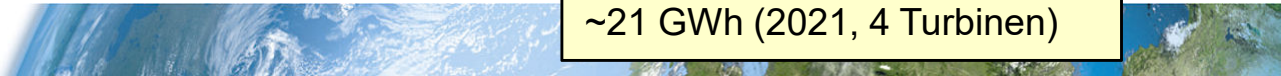
## Earth's Energy Budget (2)

The global energy inventory increased by 282 [177 to 387] Zettajoules (ZJ;  $10^{21}$  Joules) for the period 1971–2006 and 152 [100 to 205] ZJ for the period 2006–2018. This corresponds to an Earth energy imbalance of 0.50 [0.32 to 0.69]  $W m^{-2}$  for the period 1971–2006, increasing to 0.79 [0.52 to 1.06]  $W m^{-2}$  for the period 2006–2018, expressed per unit area of Earth's surface. Ocean heat uptake is by far the largest contribution and accounts for 91% of the total energy change. Compared to AR5, the contribution from land heating has been revised upwards from about 3% to about 5%. Melting of ice and warming of the atmosphere account for about 3% and 1% of the total change respectively. More comprehensive analysis of inventory components and cross-validation of global heating rates from satellite and in situ observations lead to a strengthened assessment relative to AR5 (*high confidence*). {Box 7.2, 7.2.2, Table 7.1, 7.5.2.3}

1 ZJ =  $10^{21}$  J  
 $\approx 2.78 \cdot 10^{11}$  kWh = 278 PWh

PV-Anlage Sausen: ~ 3.5 MWh

Windkraftanlage Berg:  
~21 GWh (2021, 4 Turbinen)

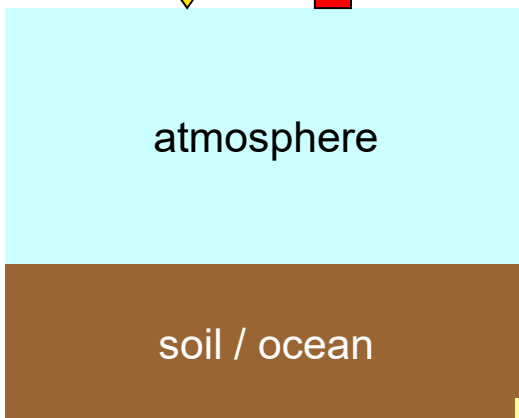
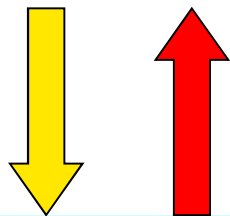


# Was ist der "Strahlungsantrieb"? (vereinfacht)

## What is "radiative forcing"? (simplified)

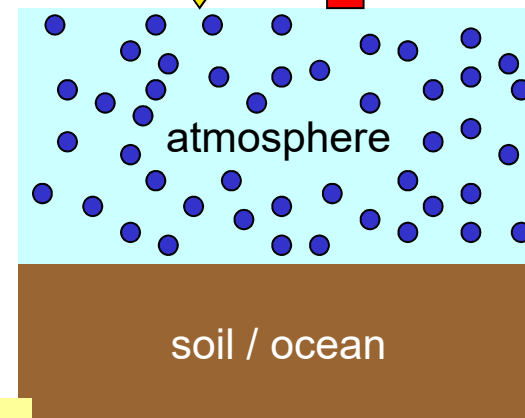
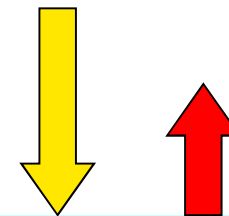
Gleichgewicht

$$RF = 0$$



Gestörte Situation

$$RF > 0 \rightarrow \Delta T \uparrow$$



$$\Delta T_{\text{surf}} = \lambda \cdot RF$$





## Schematic comparing RF calculation methodologies

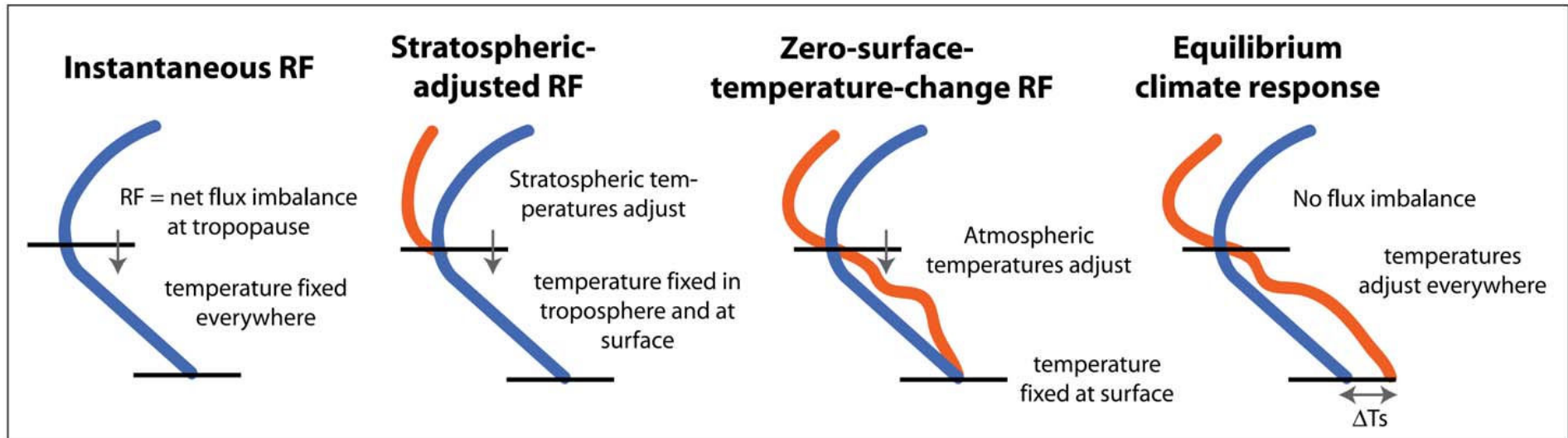


**Figure 2.2.** Schematic comparing RF calculation methodologies. Radiative forcing, defined as the net flux imbalance at the tropopause, is shown by an arrow. The horizontal lines represent the surface (lower line) and tropopause (upper line). The unperturbed temperature profile is shown as the blue line and the perturbed temperature profile as the red line. From left to right: Instantaneous RF: atmospheric temperatures are fixed everywhere; stratospheric-adjusted RF: allows stratospheric temperatures to adjust; zero-surface-temperature-change RF: allows atmospheric temperatures to adjust everywhere with surface temperatures fixed; and equilibrium climate response: allows the atmospheric and surface temperatures to adjust to reach equilibrium (no tropopause flux imbalance), giving a surface temperature change ( $\Delta T_s$ ).



## Radiative forcing (RF) and effective radiative forcing (ERF) estimates

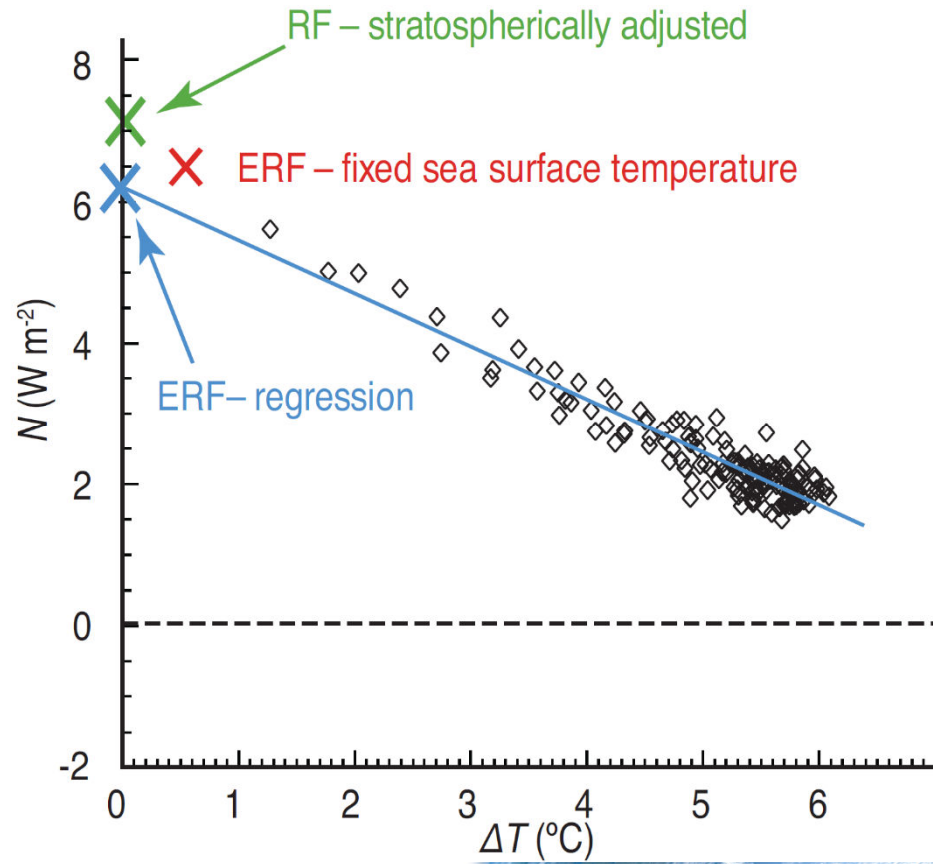
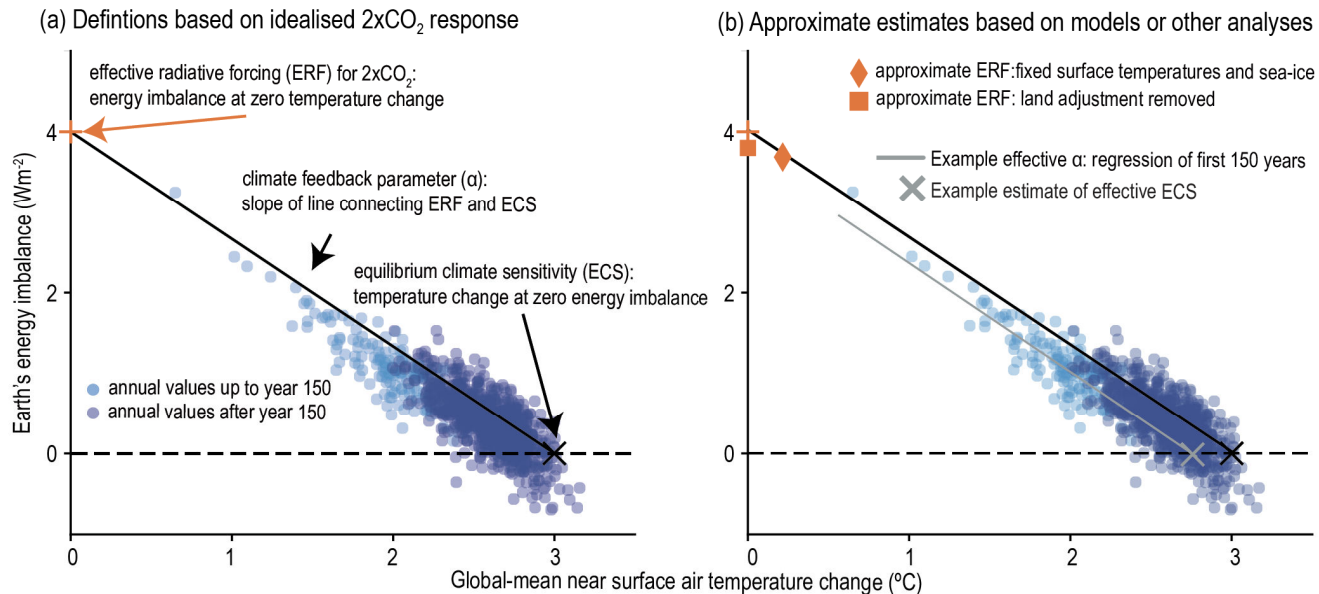


**Figure 7.2** | Radiative forcing (RF) and effective radiative forcing (ERF) estimates derived by two methods, for the example of  $4 \times \text{CO}_2$  experiments in one climate model.  $N$  is the net energy imbalance at the top of the atmosphere and  $\Delta T$  the global mean surface temperature change. The fixed sea surface temperature ERF estimate is from an atmosphere-land model averaged over 30 years. The regression estimate is from 150 years of a coupled model simulation after an instantaneous quadrupling of  $\text{CO}_2$ , with the  $N$  from individual years in this regression shown as black diamonds. The stratospherically adjusted RF is the tropopause energy imbalance from otherwise identical radiation calculations at  $1 \times$  and  $4 \times \text{CO}_2$  concentrations. (Figure follows Andrews et al., 2012.) See also Figure 8.1.

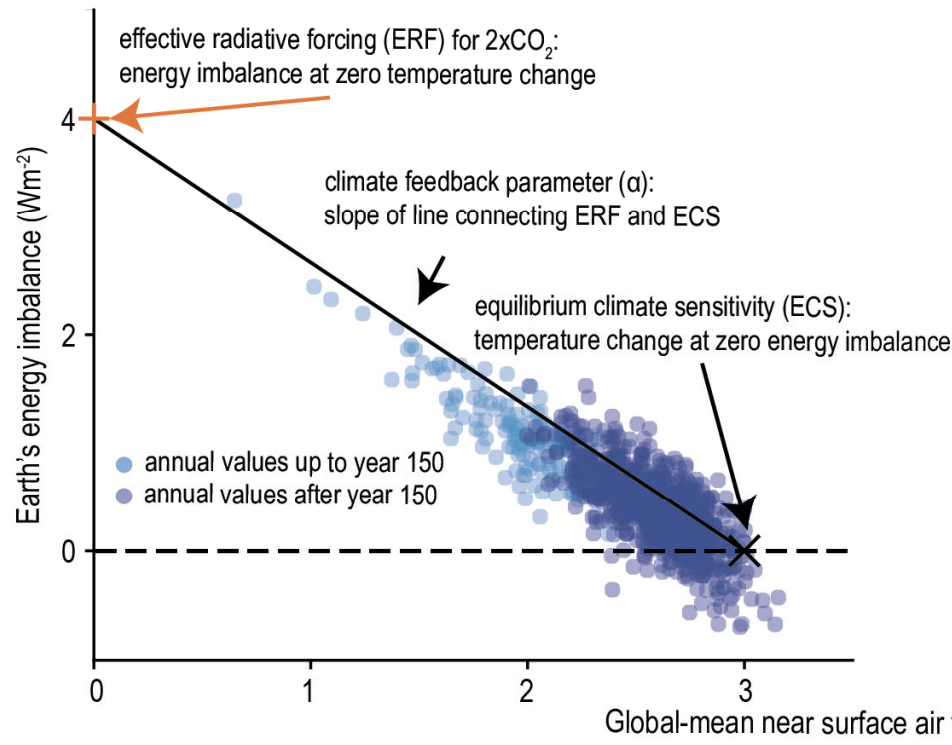
## Schematics of the forcing–feedback framework



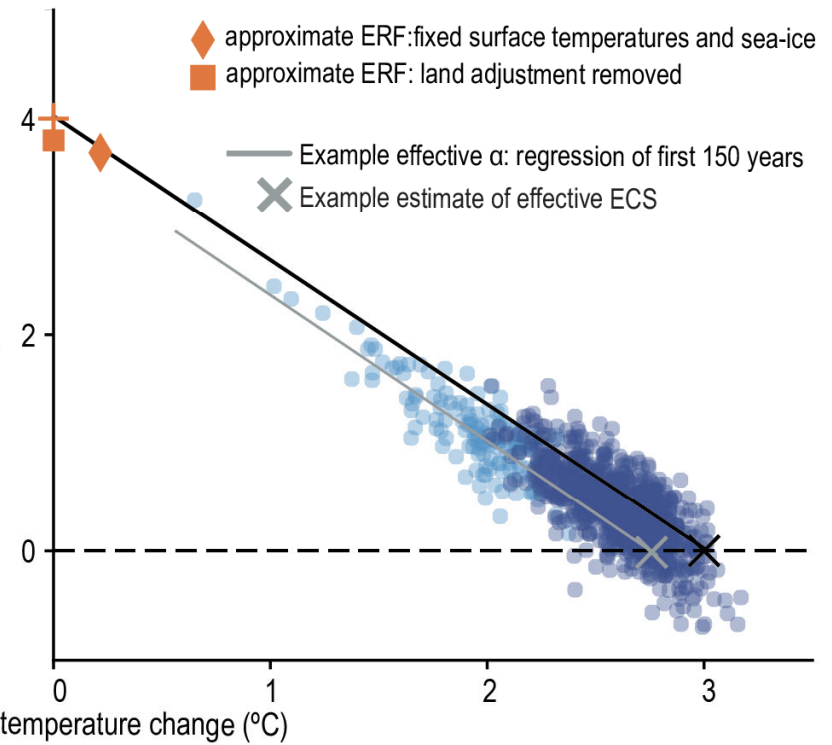
**Box 7.1, Figure 1 | Schematics of the forcing–feedback framework adopted within the assessment, following Equation 7.1.** The figure illustrates how the Earth’s top-of-atmosphere (TOA) net energy flux might evolve for a hypothetical doubling of atmospheric  $\text{CO}_2$  concentration above pre-industrial levels, where an initial positive energy imbalance (energy entering the Earth system, shown on the y-axis) is gradually restored towards equilibrium as the surface temperature warms (shown on the x-axis). **(a)** illustrates the definitions of effective radiative forcing (ERF) for the special case of a doubling of atmospheric  $\text{CO}_2$  concentration, the feedback parameter and the equilibrium climate sensitivity (ECS). **(b)** illustrates how approximate estimates of these metrics are made within the chapter and how these approximations might relate to the exact definitions adopted in panel (a).

# Schematics of the forcing–feedback framework

(a) Definitions based on idealised  $2\times\text{CO}_2$  response



(b) Approximate estimates based on models or other analyses



## Statements in the Executive Summary

### *Earth's Energy Budget (3)*

**Improved quantification of effective radiative forcing, the climate system radiative response, and the observed energy increase in the Earth system for the period 1971–2018 demonstrate improved closure of the global energy budget compared to AR5.** Combining the likely range of ERF with the central estimate of radiative response gives an expected energy gain of 340 [47 to 662] ZJ. Combining the likely range of climate response with the central estimate of ERF gives an expected energy gain of 340 [147 to 527] ZJ. Both estimates are consistent with an independent observation-based assessment of the global energy increase of 284 [96 to 471] ZJ, (*very likely* range) expressed relative to the estimated 1850–1900 Earth energy imbalance (*high confidence*). {7.2.2, Box 7.2, 7.3.5, 7.5.2}



## Anomalies in global mean all-sky top-of-atmosphere (TOA) fluxes from CERES-EBAF Ed4.0 (solid black lines) and various CMIP6 climate models (coloured lines) in terms of (a) reflected solar, (b) emitted thermal and (c) net TOA fluxes

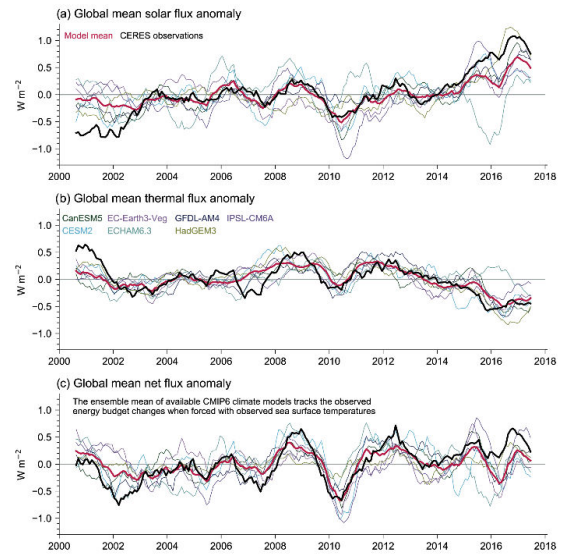
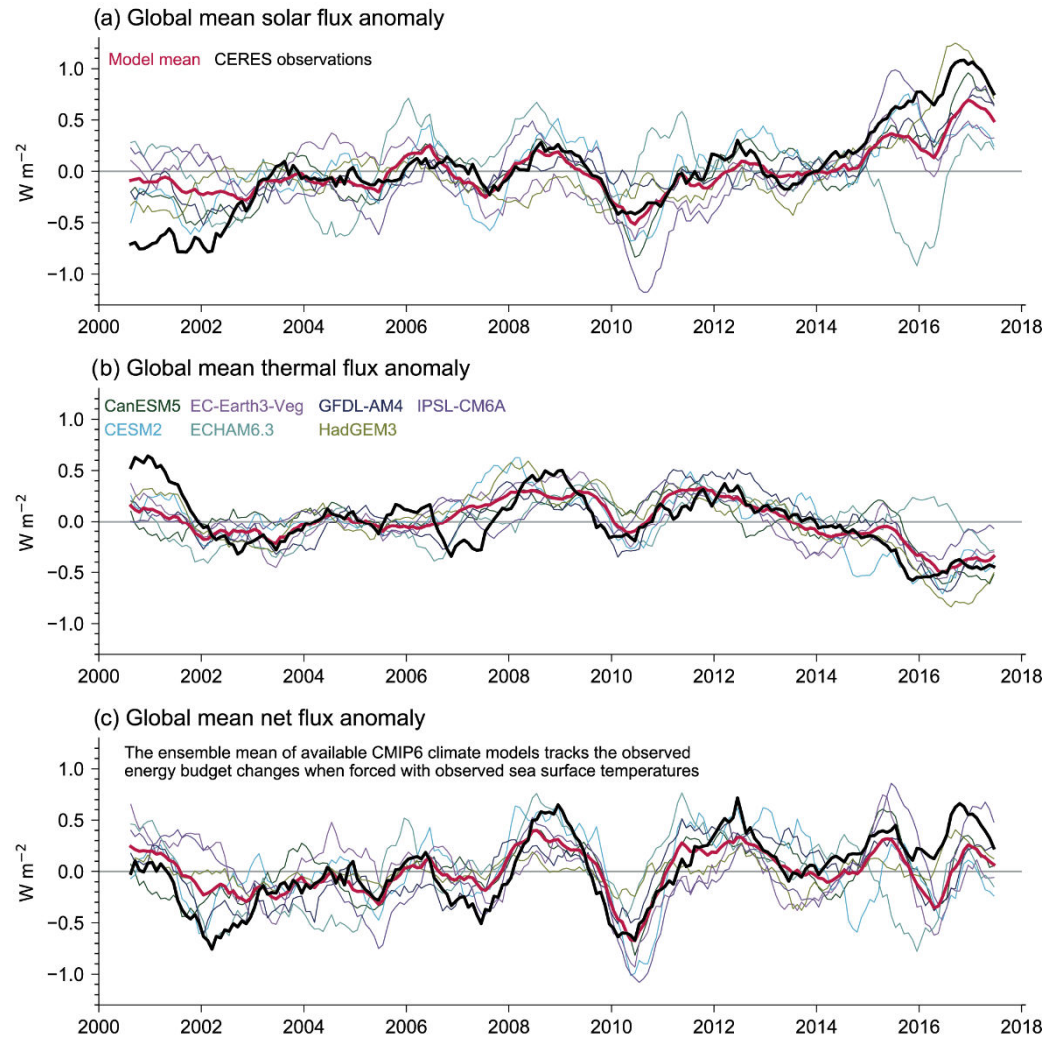


**Figure 7.3 | Anomalies in global mean all-sky top-of-atmosphere (TOA) fluxes from CERES-EBAF Ed4.0 (solid black lines) and various CMIP6 climate models (coloured lines) in terms of (a) reflected solar, (b) emitted thermal and (c) net TOA fluxes.** The multi-model means are additionally depicted as solid red lines. Model fluxes stem from simulations driven with prescribed sea surface temperatures (SSTs) and all known anthropogenic and natural forcings. Shown are anomalies of 12-month running means. All flux anomalies are defined as positive downwards, consistent with the sign convention used throughout this chapter. The correlations between the multi-model means (solid red lines) and the CERES records (solid black lines) for 12-month running means are: 0.85 for the global mean reflected solar; 0.73 for outgoing thermal radiation; and 0.81 for net TOA radiation. Figure adapted from Loeb et al. (2020). Further details on data sources and processing are available in the chapter data table (Table 7.SM.14).



## Statements in the Executive Summary

### *Earth's Energy Budget (4)*

Since AR5, additional evidence for a widespread decline (or dimming) in solar radiation reaching the surface is found in the observational records between the 1950s and 1980s, with a partial recovery (brightening) at many observational sites thereafter (*high confidence*). These trends are neither a local phenomenon nor a measurement artefact (*high confidence*). Multi-decadal variation in anthropogenic aerosol emissions are thought to be a major contributor (*medium confidence*), but multi-decadal variability in cloudiness may also have played a role. The downward and upward thermal radiation at the surface has increased in recent decades, in line with increased greenhouse gas concentrations and associated surface and atmospheric warming and moistening (*medium confidence*). {7.2.2}





## Contributions of the different components of the global energy inventory

**Table 7.1 | Contributions of the different components of the global energy inventory for the periods 1971–2018, 1993–2018 and 2006–2018 (Box 7.2 and Cross-Chapter Box 9.1).** Energy changes are computed as the difference between annual mean values or year mid-points. The total heating rates correspond to Earth’s energy imbalance and are expressed per unit area of Earth’s surface.

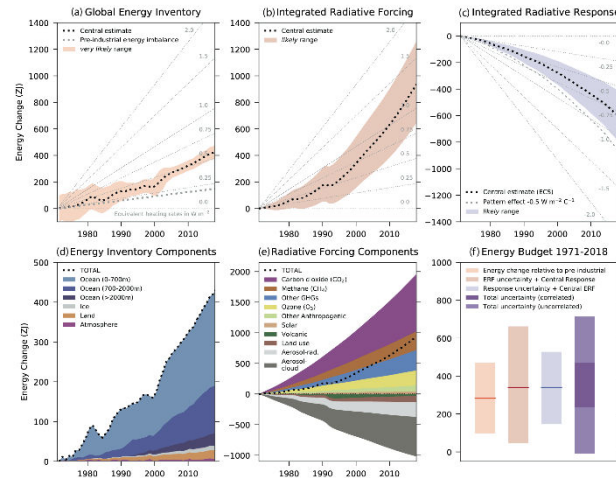
Component	1971–2018		1993–2018		2006–2018	
	Energy Gain (ZJ)	%	Energy Gain (ZJ)	%	Energy Gain (ZJ)	%
Ocean	396.0 [285.7 to 506.2]	91.0	263.0 [194.1 to 331.9]	91.0	138.8 [86.4 to 191.3]	91.1
0–700 m	241.6 [162.7 to 320.5]	55.6	151.5 [114.1 to 188.9]	52.4	75.4 [48.7 to 102.0]	49.5
700–2000 m	123.3 [96.0 to 150.5]	28.3	82.8 [59.9 to 105.6]	28.6	49.7 [29.0 to 70.4]	32.6
>2000 m	31.0 [15.7 to 46.4]	7.1	28.7 [14.5 to 43.0]	10.0	13.8 [7.0 to 20.6]	9.0
Land	21.8 [18.6 to 25.0]	5.0	13.7 [12.4 to 14.9]	4.7	7.2 [6.6 to 7.8]	4.7
Cryosphere	11.5 [9.0 to 14.0]	2.7	8.8 [7.0 to 10.5]	3.0	4.7 [3.3 to 6.2]	3.1
Atmosphere	5.6 [4.6 to 6.7]	1.3	3.8 [3.2 to 4.3]	1.3	1.6 [1.2 to 2.1]	1.1
<b>TOTAL</b>	<b>434.9 [324.5 to 545.3] ZJ</b>		<b>289.2 [220.3 to 358.1] ZJ</b>		<b>152.4 [100.0 to 204.9] ZJ</b>	
<b>Heating Rate</b>	<b>0.57 [0.43 to 0.72] W m<sup>-2</sup></b>		<b>0.72 [0.55 to 0.89] W m<sup>-2</sup></b>		<b>0.79 [0.52 to 1.06] W m<sup>-2</sup></b>	

## Contributions of the different components of the global energy inventory

**Table 7.1 | Contributions of the different components of the global energy inventory for the periods 1971–2018, 1993–2018 and 2006–2018 (Box 7.2 and Cross-Chapter Box 9.1).** Energy changes are computed as the difference between annual mean values or year mid-points. The total heating rates correspond to Earth's energy imbalance and are expressed per unit area of Earth's surface.

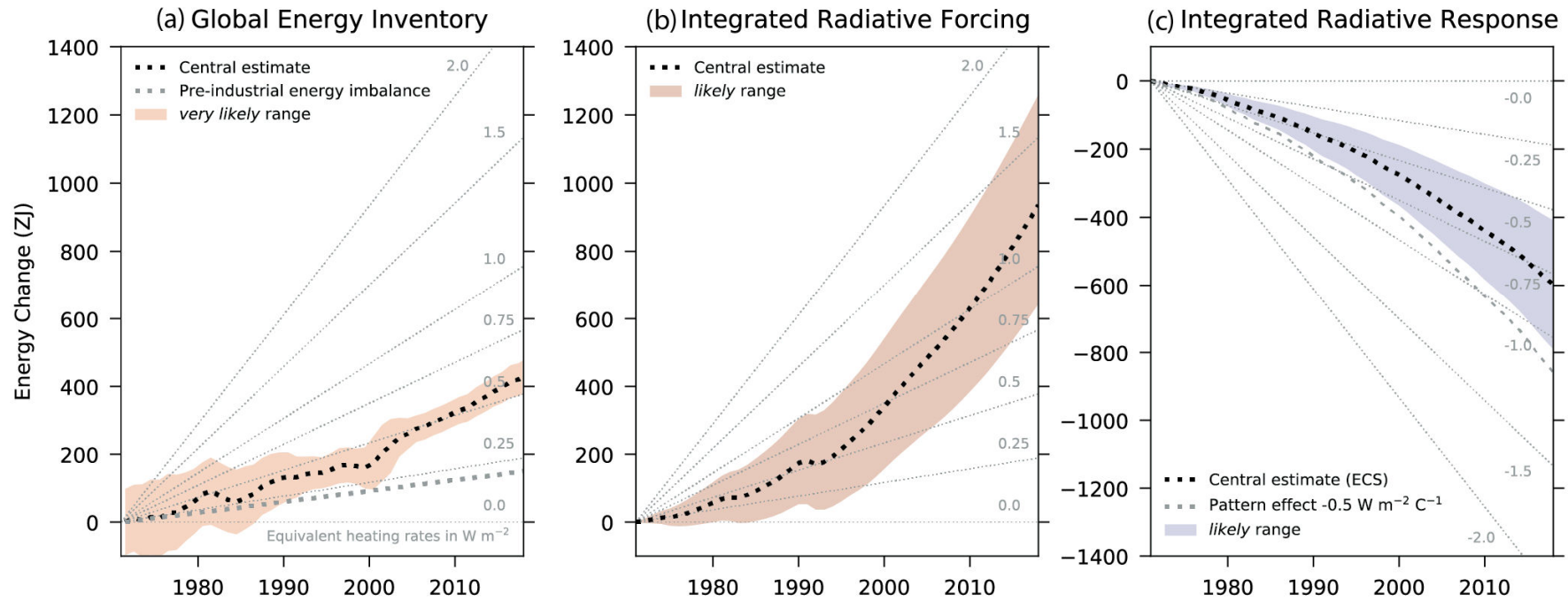
Component	1971–2018		2006–2018	
	Energy Gain (ZJ)	%	Energy Gain (ZJ)	%
Ocean	396.0 [285.7 to 506.2]	91.0	138.8 [86.4 to 191.3]	91.1
0–700 m	241.6 [162.7 to 320.5]	55.6	75.4 [48.7 to 102.0]	49.5
700–2000 m	123.3 [96.0 to 150.5]	28.3	49.7 [29.0 to 70.4]	32.6
>2000 m	31.0 [15.7 to 46.4]	7.1	13.8 [7.0 to 20.6]	9.0
Land	21.8 [18.6 to 25.0]	5.0	7.2 [6.6 to 7.8]	4.7
Cryosphere	11.5 [9.0 to 14.0]	2.7	4.7 [3.3 to 6.2]	3.1
Atmosphere	5.6 [4.6 to 6.7]	1.3	1.6 [1.2 to 2.1]	1.1
<b>TOTAL</b>	<b>434.9 [324.5 to 545.3] ZJ</b>		<b>152.4 [100.0 to 204.9] ZJ</b>	
<b>Heating Rate</b>	<b>0.57 [0.43 to 0.72] W m<sup>-2</sup></b>		<b>0.79 [0.52 to 1.06] W m<sup>-2</sup></b>	

# Estimates of the net cumulative energy change for the period 1971–2018

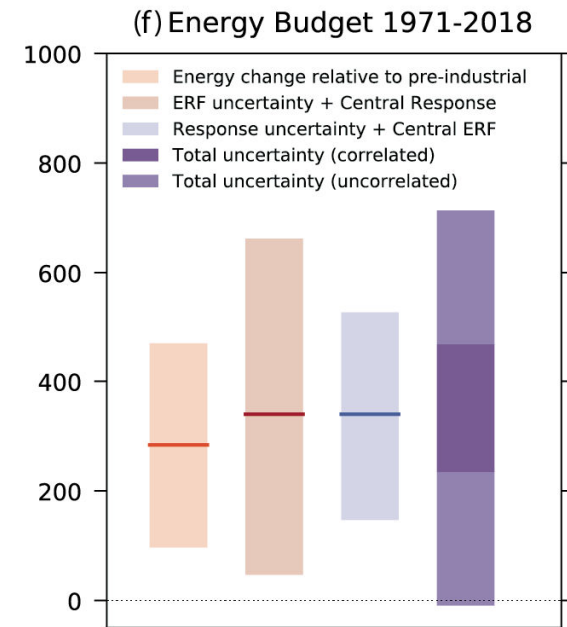
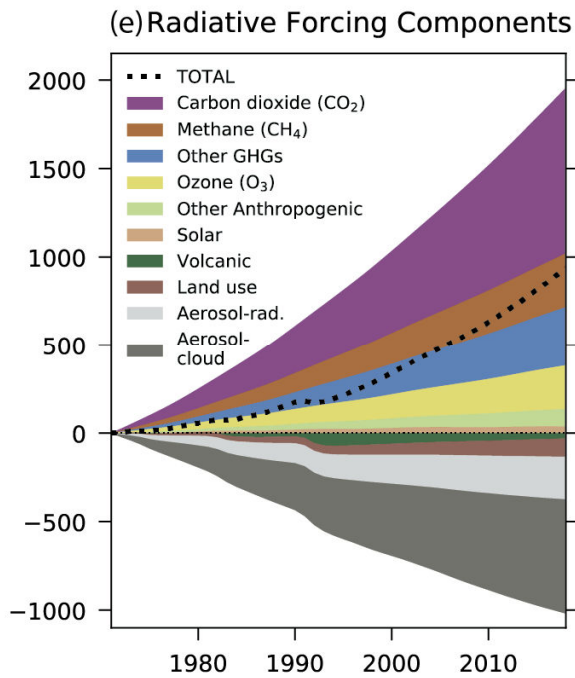
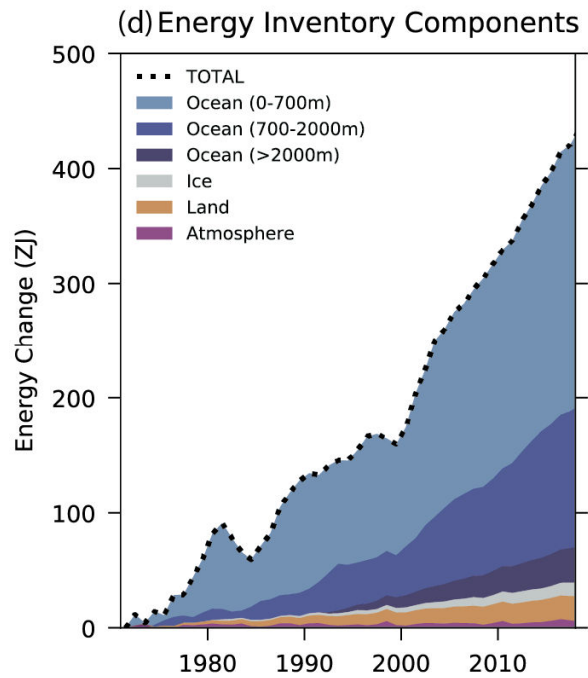


**Box 7.2, Figure 1 | Estimates of the net cumulative energy change ( $ZJ = 10^{21}$  Joules) for the period 1971–2018 associated with: (a) observations of changes in the global energy inventory; (b) integrated radiative forcing; and (c) integrated radiative response.** Black dotted lines indicate the central estimate with *likely* and *very likely* ranges as indicated in the legend. The grey dotted lines indicate the energy change associated with an estimated pre-industrial Earth energy imbalance of  $0.2 \text{ W m}^{-2}$  (a), and an illustration of an assumed pattern effect of  $-0.5 \text{ W m}^{-2} \text{ } ^\circ\text{C}^{-1}$  (c). Background grey lines indicate equivalent heating rates in  $\text{W m}^{-2}$  per unit area of Earth’s surface. Panels (d) and (e) show the breakdown of components, as indicated in the legend, for the global energy inventory and integrated radiative forcing, respectively. Panel (f) shows the global energy budget assessed for the period 1971–2018, that is, the consistency between the change in the global energy inventory relative to pre-industrial and the implied energy change from integrated radiative forcing plus integrated radiative response under a number of different assumptions, as indicated in the legend, including assumptions of correlated and uncorrelated uncertainties in forcing plus response. Shading represents the *very likely* range for observed energy change relative to pre-industrial levels and *likely* range for all other quantities. Forcing and response time series are expressed relative to a baseline period of 1850–1900. Further details on data sources and processing are available in the chapter data table (Table 7.SM.14).

# Estimates of the net cumulative energy change for the period 1971–2018



# Estimates of the net cumulative energy change for the period 1971–2018



## Statements in the Executive Summary

### *Effective Radiative Forcing (1)*

For carbon dioxide, methane, nitrous oxide and chlorofluorocarbons, there is now evidence to quantify the effect on ERF of tropospheric adjustments (e.g., from changes in atmospheric temperatures, clouds and water vapour). The assessed ERF for a doubling of carbon dioxide compared to 1750 levels ( $3.93 \pm 0.47 \text{ W m}^{-2}$ ) is larger than in AR5. Effective radiative forcings (ERF), introduced in AR5, have been estimated for a larger number of agents and shown to be more closely related to the temperature response than the stratospheric-temperature adjusted radiative forcing. For carbon dioxide, the adjustments include the physiological effects on vegetation (*high confidence*). {7.3.2}



## Schematic comparing RF calculation methodologies

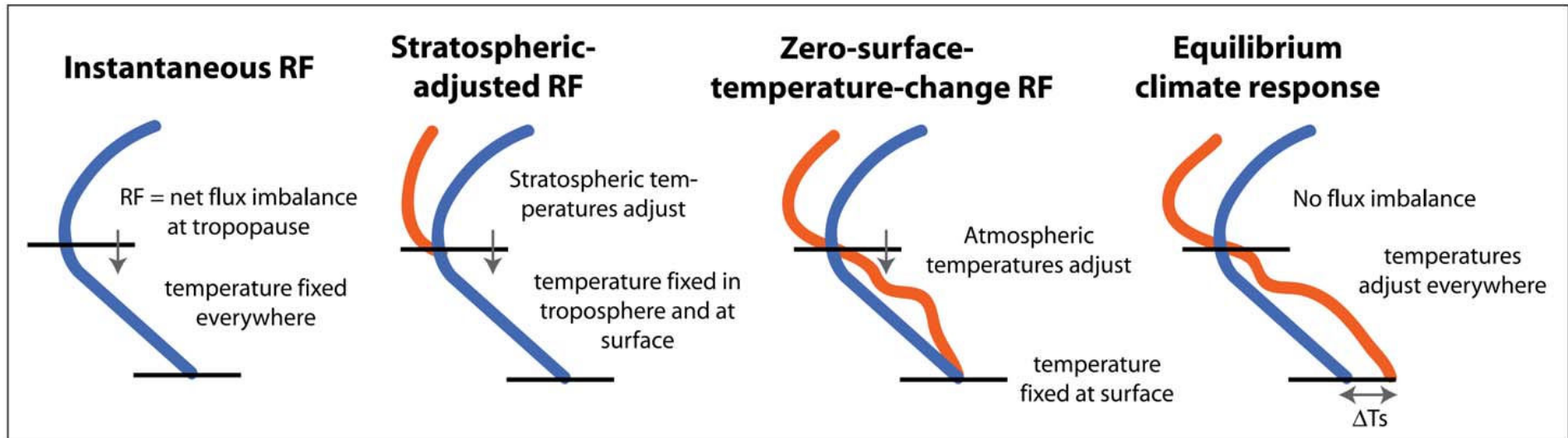


**Figure 2.2.** Schematic comparing RF calculation methodologies. Radiative forcing, defined as the net flux imbalance at the tropopause, is shown by an arrow. The horizontal lines represent the surface (lower line) and tropopause (upper line). The unperturbed temperature profile is shown as the blue line and the perturbed temperature profile as the red line. From left to right: Instantaneous RF: atmospheric temperatures are fixed everywhere; stratospheric-adjusted RF: allows stratospheric temperatures to adjust; zero-surface-temperature-change RF: allows atmospheric temperatures to adjust everywhere with surface temperatures fixed; and equilibrium climate response: allows the atmospheric and surface temperatures to adjust to reach equilibrium (no tropopause flux imbalance), giving a surface temperature change ( $\Delta T_s$ ).



## Radiative adjustments at top of atmosphere for seven different climate drivers as a proportion of forcing

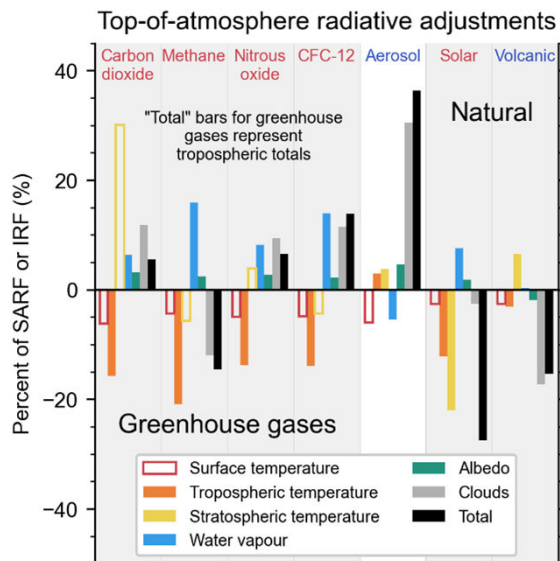


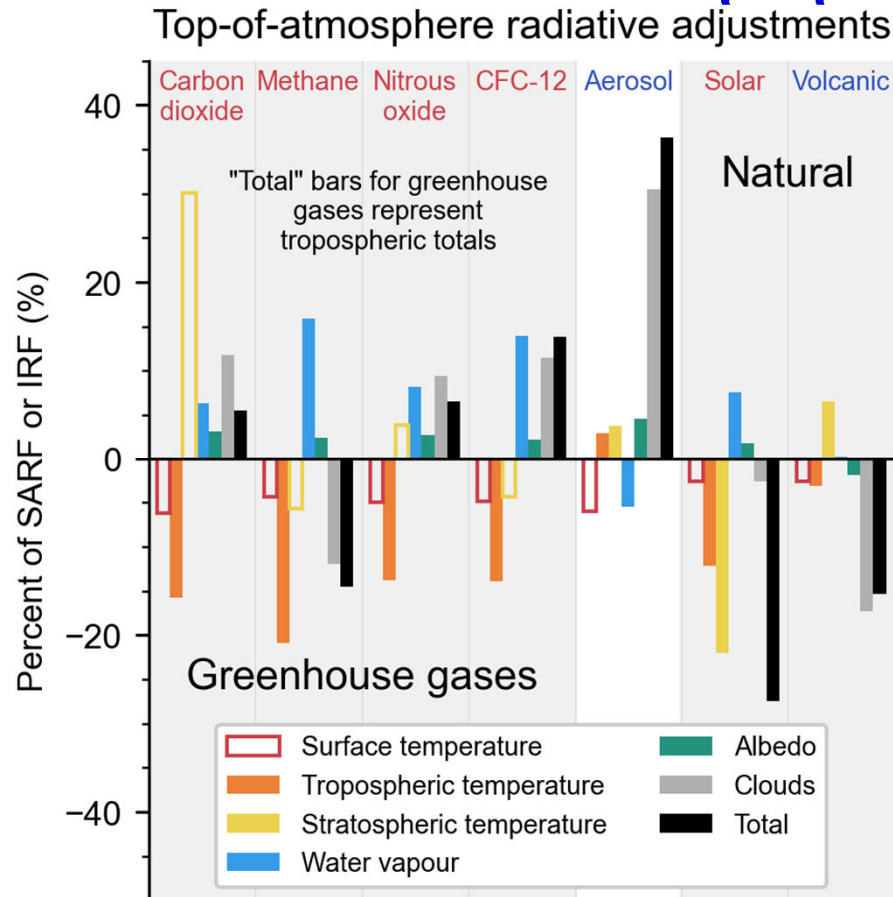
**Figure 7.4 | Radiative adjustments at top of atmosphere for seven different climate drivers as a proportion of forcing.** Tropospheric temperature (orange), stratospheric temperature (yellow), water vapour (blue), surface albedo (green), clouds (grey) and the total adjustment (black) is shown. For the greenhouse gases (carbon dioxide, methane, nitrous oxide and CFC-12) the adjustments are expressed as a percentage of stratospheric-temperature-adjusted radiative forcing (SARF), whereas for aerosol, solar and volcanic forcing they are expressed as a percentage of instantaneous radiative forcing (IRF). Land surface temperature response (outline red bar) is shown, but included in the definition of forcing. Data from Smith et al. (2018b) for carbon dioxide and methane; Smith et al. (2018b) and Gray et al. (2009) for solar; Hodnebrog et al. (2020b) for nitrous oxide and CFC-12; Smith et al. (2020b) for aerosol, and Marshall et al. (2020) for volcanic. Further details on data sources and processing are available in the chapter data table (Table 7.SM.14).

IPCC 2013, Chap. 7





# Radiative adjustments at top of atmosphere for seven different climate drivers as a proportion of forcing



IPCC 2013, Chap. 7



## Statements in the Executive Summary

### *Effective Radiative Forcing (2)*

The total anthropogenic ERF over the industrial era (1750–2019) was 2.72 [1.96 to 3.48]  $\text{W m}^{-2}$ . This estimate has increased by 0.43  $\text{W m}^{-2}$  compared to AR5 estimates for 1750–2011. This increase includes +0.34  $\text{W m}^{-2}$  from increases in atmospheric concentrations of well-mixed greenhouse gases (including halogenated species) since 2011, +0.15  $\text{W m}^{-2}$  from upwards revisions of their radiative efficiencies and +0.10  $\text{W m}^{-2}$  from re-evaluation of the ozone and stratospheric water vapour ERF. The 0.59  $\text{W m}^{-2}$  increase in ERF from greenhouse gases is partly offset by a better-constrained assessment of total aerosol ERF that is more strongly negative than in AR5, based on multiple lines of evidence (*high confidence*). Changes in surface reflectance from land-use change, deposition of light-absorbing particles on ice and snow, and contrails and aviation-induced cirrus have also contributed to the total anthropogenic ERF over the industrial era, with  $-0.20$  [ $-0.30$  to  $-0.10$ ]  $\text{W m}^{-2}$  (*medium confidence*), +0.08 [0 to 0.18]  $\text{W m}^{-2}$  (low confidence) and +0.06 [0.02 to 0.10]  $\text{W m}^{-2}$  (*low confidence*), respectively. {7.3.2, 7.3.4, 7.3.5}



## Statements in the Executive Summary

### *Effective Radiative Forcing (3)*

**Anthropogenic emissions of greenhouse gases and their precursors contribute an ERF of 3.84 [3.46 to 4.22] W m<sup>-2</sup> over the industrial era (1750–2019). Most of this total ERF, 3.32 [3.03 to 3.61] W m<sup>-2</sup>, comes from the well-mixed greenhouse gases, with changes in ozone and stratospheric water vapour (from methane oxidation) contributing the remainder.** The ERF of greenhouse gases is composed of 2.16 [1.90 to 2.41] W m<sup>-2</sup> from carbon dioxide, 0.54 [0.43 to 0.65] W m<sup>-2</sup> from methane, 0.41 [0.33 to 0.49] W m<sup>-2</sup> from halogenated species, and 0.21 [0.18 to 0.24] W m<sup>-2</sup> from nitrous oxide. The ERF for ozone is 0.47 [0.24 to 0.71] W m<sup>-2</sup>. The estimate of ERF for ozone has increased since AR5 due to revised estimates of precursor emissions and better accounting for effects of tropospheric ozone precursors in the stratosphere. The estimated ERF for methane has slightly increased due to a combination of increases from improved spectroscopic treatments being somewhat offset by accounting for adjustments (*high confidence*). {7.3.2, 7.3.5}



# Present-day mole fractions [ppt] and effective radiative forcing [W m<sup>-2</sup>] for the well-mixed greenhouse gases

**Table 7.5 | Present-day mole fractions in parts per trillion (pmol mol<sup>-1</sup>), except where specified, and effective radiative forcing (ERF, in W m<sup>-2</sup>) for the well-mixed greenhouse gases (WMGHGs).** Data taken from Chapter 2 (Section 2.2.3). The data for 2011 (the time of the AR5 estimates) are also shown. Some of the concentrations vary slightly from those reported in AR5 owing to averaging different data sources. Individual species are reported where 1750–2019 ERF is at least 0.001 W m<sup>-2</sup>. Radiative efficiencies for the minor gases are given in Supplementary Material, Table 7.SM.7. Uncertainties in the ERF for all gases are dominated by the uncertainties in the radiative efficiencies. Tabulated global mixing ratios of all WMGHGs and ERFs from 1750 to 2019 are provided in Annex III.

	Concentration				ERF with Respect to 1850		ERF with Respect to 1750	
	2019	2011	1850	1750	2019	2011	2019	2011
CO <sub>2</sub> (ppm)	409.9	390.5	285.5	278.3	2.012 ± 0.241	1.738	2.156 ± 0.259	1.882
CH <sub>4</sub> (ppb)	1866.3	1803.3	807.6	729.2	0.496 ± 0.099	0.473	0.544 ± 0.109	0.521
N <sub>2</sub> O (ppb)	332.1	324.4	272.1	270.1	0.201 ± 0.030	0.177	0.208 ± 0.031	0.184
HFC-134a	107.6	62.7	0.0	0.0	0.018	0.010	0.018	0.010
HFC-23	32.4	24.1	0.0	0.0	0.006	0.005	0.006	0.005
HFC-32	20.0	4.7	0.0	0.0	0.002	0.001	0.002	0.001
HFC-125	29.4	10.3	0.0	0.0	0.007	0.002	0.007	0.002
HFC-143a	24.0	12.0	0.0	0.0	0.004	0.002	0.004	0.002
SF <sub>6</sub>	10.0	7.3	0.0	0.0	0.006	0.004	0.006	0.004
CF <sub>4</sub>	85.5	79.0	34.0	34.0	0.005	0.004	0.005	0.004
C <sub>2</sub> F <sub>6</sub>	4.8	4.2	0.0	0.0	0.001	0.001	0.001	0.001
CFC-11	226.2	237.3	0.0	0.0	0.066	0.070	0.066	0.070
CFC-12	503.1	528.6	0.0	0.0	0.180	0.189	0.180	0.189
CFC-113	69.8	74.6	0.0	0.0	0.021	0.022	0.021	0.022
CFC-114	16.0	16.3	0.0	0.0	0.005	0.005	0.005	0.005
CFC-115	8.7	8.4	0.0	0.0	0.002	0.002	0.002	0.002
HCFC-22	246.8	213.2	0.0	0.0	0.053	0.046	0.053	0.046
HCFC-141b	24.4	21.4	0.0	0.0	0.004	0.003	0.004	0.003
HCFC-142b	22.3	21.2	0.0	0.0	0.004	0.004	0.004	0.004
CCl <sub>4</sub>	77.9	86.1	0.0	0.0	0.013	0.014	0.013	0.014
Sum of HFCs (HFC-134a equivalent)	237.1	128.6	0.0	0.0	0.040	0.022	0.040	0.022
Sum of CFCs+HCFCs+other ozone depleting gases covered by the Montreal Protocol (CFC-12 equivalent)	1031.9	1050.1	0.0	0.0	0.354	0.362	0.354	0.362
Sum of PFCs (CF <sub>4</sub> equivalent)	109.4	98.9	34.0	34.0	0.007	0.006	0.007	0.006
Sum of Halogenated species					0.408 ± 0.078	0.394	0.408 ± 0.078	0.394
Total					3.118 ± 0.258	2.782	3.317 ± 0.278	2.981

IPCC 2013, Chap. 7



## Present-day mole fractions [ppt] and effective radiative forcing [W m<sup>-2</sup>] for the well-mixed greenhouse gases

	Concentration				ERF with Respect to 1850		ERF with Respect to 1750	
	2019	2011	1850	1750	2019	2011	2019	2011
CO <sub>2</sub> (ppm)	409.9	390.5	285.5	278.3	2.012 ± 0.241	1.738	2.156 ± 0.259	1.882
CH <sub>4</sub> (ppb)	1866.3	1803.3	807.6	729.2	0.496 ± 0.099	0.473	0.544 ± 0.109	0.521
N <sub>2</sub> O (ppb)	332.1	324.4	272.1	270.1	0.201 ± 0.030	0.177	0.208 ± 0.031	0.184
HFC-134a	107.6	62.7	0.0	0.0	0.018	0.010	0.018	0.010
Sum of halogenated species					0.406 ± 0.076	0.394	0.406 ± 0.076	0.394
Total					3.118 ± 0.258	2.782	3.317 ± 0.278	2.981



## Statements in the Executive Summary

### *Effective Radiative Forcing (4)*

**Aerosols contribute an ERF of  $-1.3$  [ $-2.0$  to  $-0.6$ ]  $\text{W m}^{-2}$  over the industrial era (1750–2014) (*medium confidence*). The ERF due to aerosol–cloud interactions (ERF<sub>aci</sub>) contributes most to the magnitude of the total aerosol ERF (*high confidence*) and is assessed to be  $-1.0$  [ $-1.7$  to  $-0.3$ ]  $\text{W m}^{-2}$  (*medium confidence*), with the remainder due to aerosol–radiation interactions (ERF<sub>ari</sub>), assessed to be  $-0.3$  [ $-0.6$  to  $0.0$ ]  $\text{W m}^{-2}$  (*medium confidence*). There has been an increase in the estimated magnitude but a reduction in the uncertainty of the total aerosol ERF relative to AR5, supported by a combination of increased process-understanding and progress in modelling and observational analyses. ERF estimates from these separate lines of evidence are now consistent with each other, in contrast to AR5, and support the assessment that it is *virtually certain* that the total aerosol ERF is negative. Compared to AR5, the assessed magnitude of ERF<sub>aci</sub> has increased, while the magnitude of ERF<sub>ari</sub> has decreased. The total aerosol ERF over the period 1750–2019 is less certain than the headline statement assessment. It is also assessed to be smaller in magnitude at  $-1.1$  [ $-1.7$  to  $-0.4$ ]  $\text{W m}^{-2}$ , primarily due to recent emissions changes (*medium confidence*). {7.3.3, 7.3.5, 2.2.6}**

IPCC 2021, Chap. 7



# Change in effective radiative forcing (ERF) from 1750 to 2019

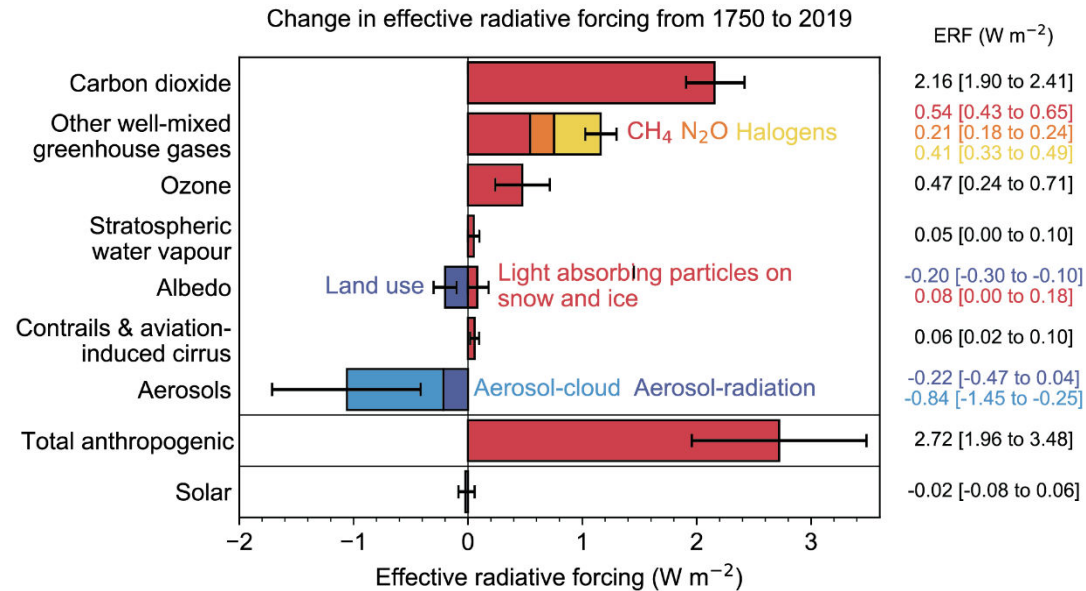
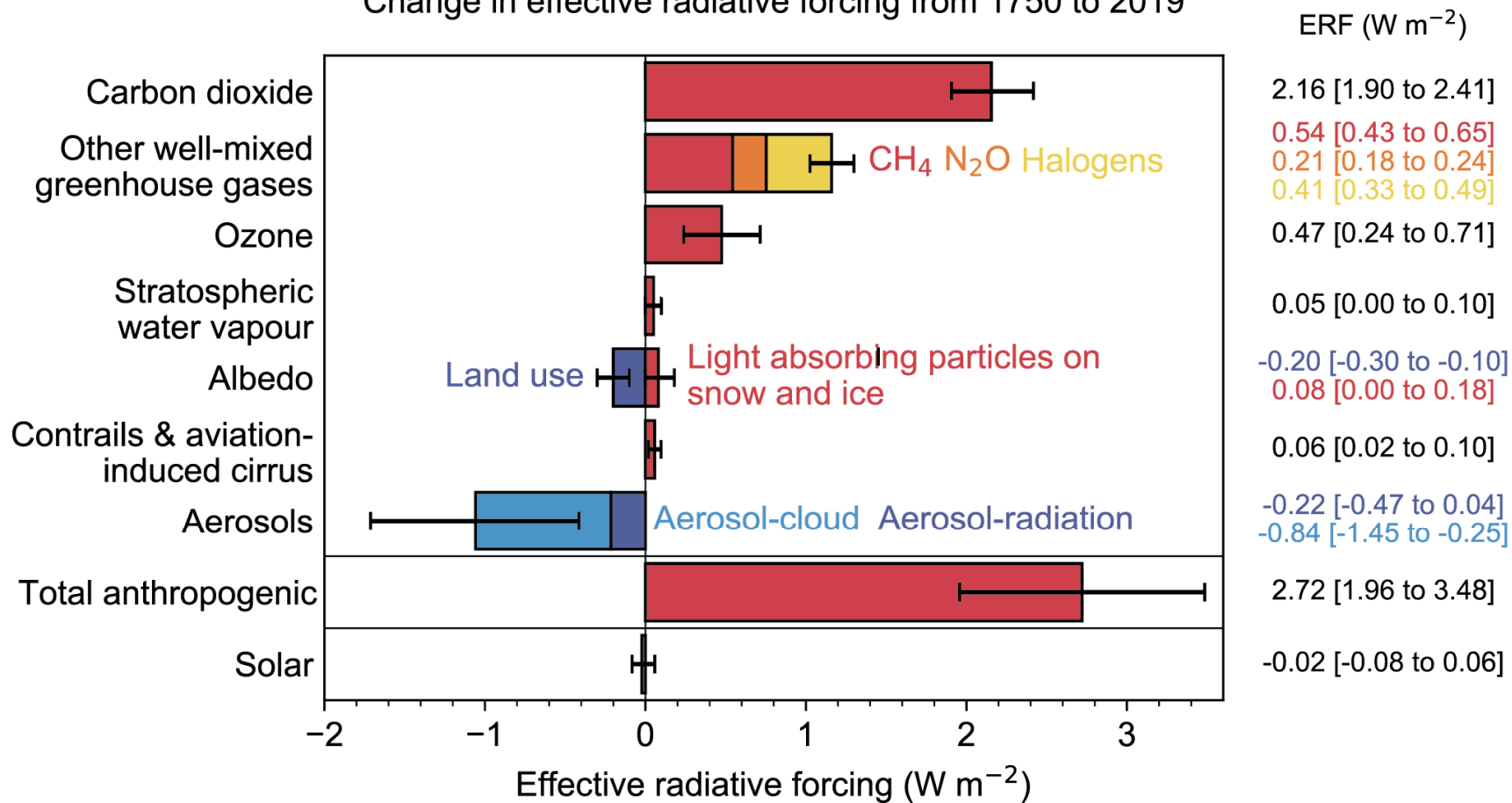


**Figure 7.6 | Change in effective radiative forcing (ERF) from 1750 to 2019 by contributing forcing agents (carbon dioxide, other well-mixed greenhouse gases (WMGHGs), ozone, stratospheric water vapour, surface albedo, contrails and aviation-induced cirrus, aerosols, anthropogenic total, and solar).** Solid bars represent best estimates, and *very likely* (5–95%) ranges are given by error bars. Non-CO<sub>2</sub> WMGHGs are further broken down into contributions from methane (CH<sub>4</sub>), nitrous oxide (N<sub>2</sub>O) and halogenated compounds. Surface albedo is broken down into land-use changes and light-absorbing particles on snow and ice. Aerosols are broken down into contributions from aerosol–cloud interactions (ERF<sub>aci</sub>) and aerosol–radiation interactions (ERF<sub>ari</sub>). For aerosols and solar, the 2019 single-year values are given (Table 7.8), which differ from the headline assessments in both cases. Volcanic forcing is not shown due to the episodic nature of volcanic eruptions. Further details on data sources and processing are available in the chapter data table (Table 7.SM.14).



### Change in effective radiative forcing from 1750 to 2019





# Contribution of forcing agents to 2019 temperature change

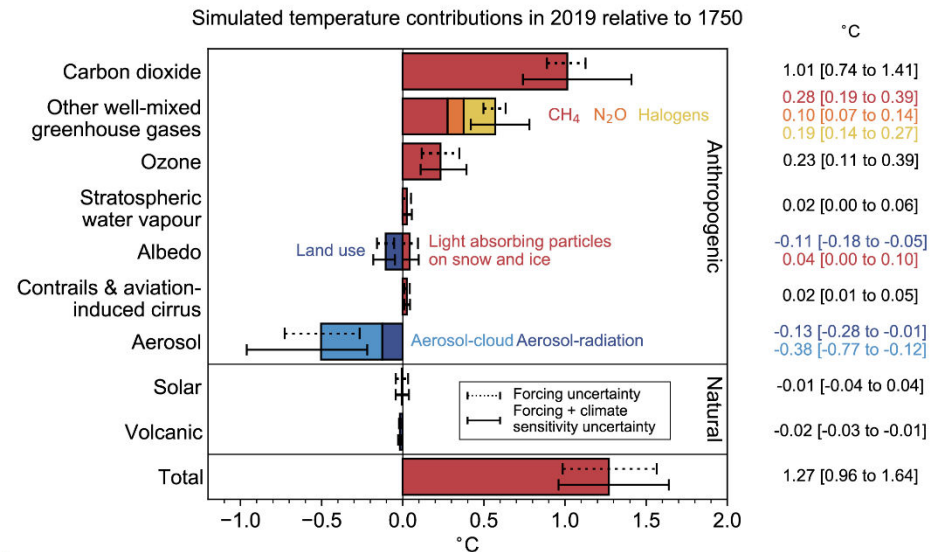
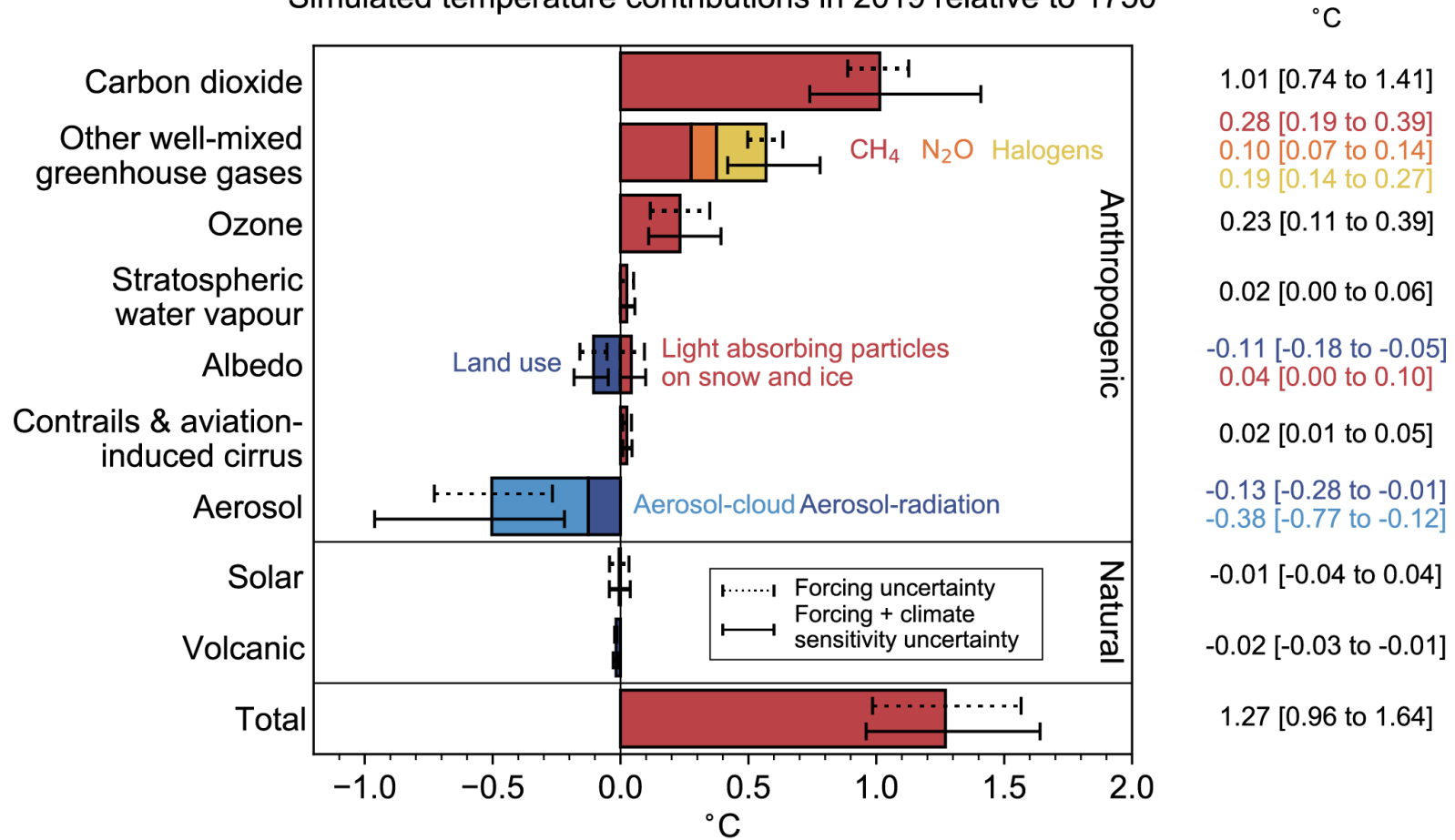


**Figure 7.7 | The contribution of forcing agents to 2019 temperature change relative to 1750 produced using the two-layer emulator (Supplementary Material 7.SM.2), constrained to assessed ranges for key climate metrics described in Cross-Chapter Box 7.1.** The results are from a 2237-member ensemble. Temperature contributions are expressed for carbon dioxide, other well-mixed greenhouse gases (WMGHGs), ozone, stratospheric water vapour, surface albedo, contrails and aviation-induced cirrus, aerosols, solar, volcanic, and total. Solid bars represent best estimates, and *very likely* (5–95%) ranges are given by error bars. Dashed error bars show the contribution of forcing uncertainty alone, using best estimates of ECS (3.0°C), TCR (1.8°C) and two-layer model parameters representing the CMIP6 multi-model mean. Solid error bars show the combined effects of forcing and climate response uncertainty using the distribution of ECS and TCR from Tables 7.13 and 7.14, and the distribution of calibrated model parameters from 44 CMIP6 models. Non-CO<sub>2</sub> WMGHGs are further broken down into contributions from methane (CH<sub>4</sub>), nitrous oxide (N<sub>2</sub>O) and halogenated compounds. Surface albedo is broken down into land-use changes and light-absorbing particles on snow and ice. Aerosols are broken down into contributions from aerosol–cloud interactions (ERF<sub>aci</sub>) and aerosol–radiation interactions (ERF<sub>ari</sub>). Further details on data sources and processing are available in the chapter data table (Table 7.SM.14).



## Simulated temperature contributions in 2019 relative to 1750



## Attributed global surface air temperature change (GSAT) from 1750 to 2019

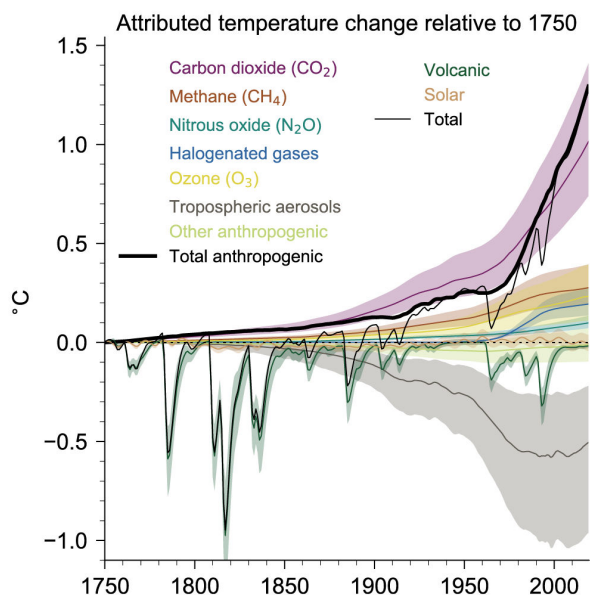
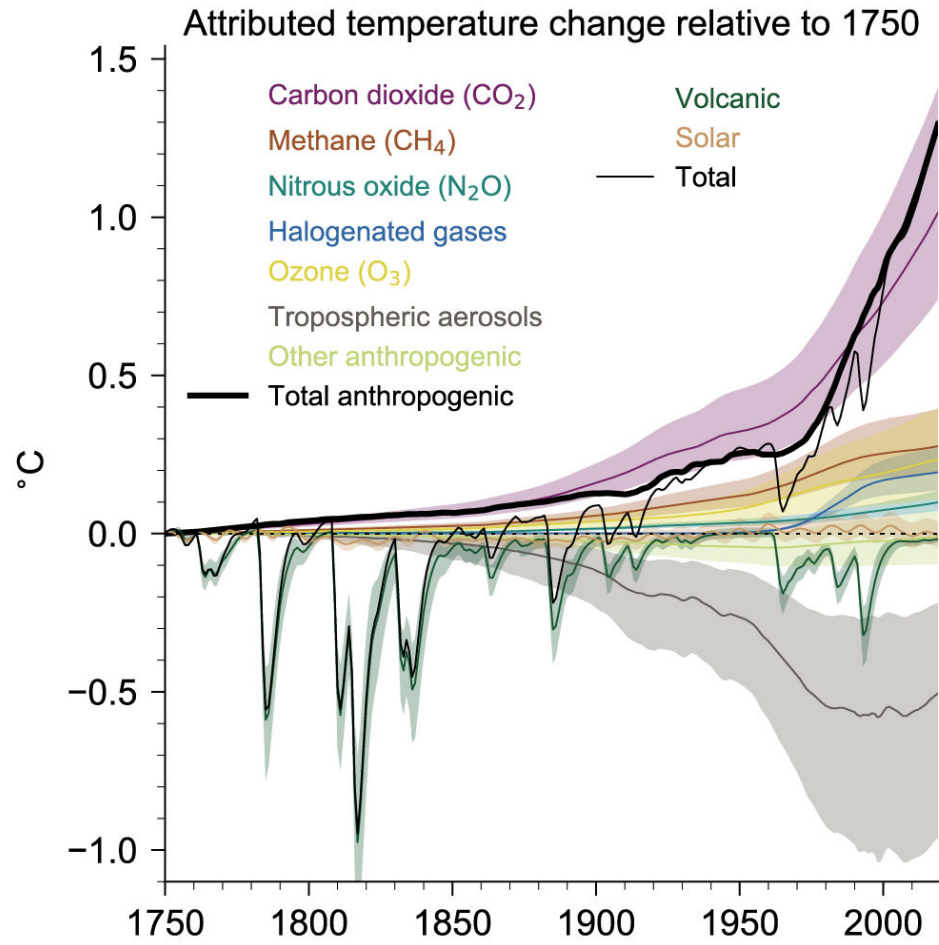


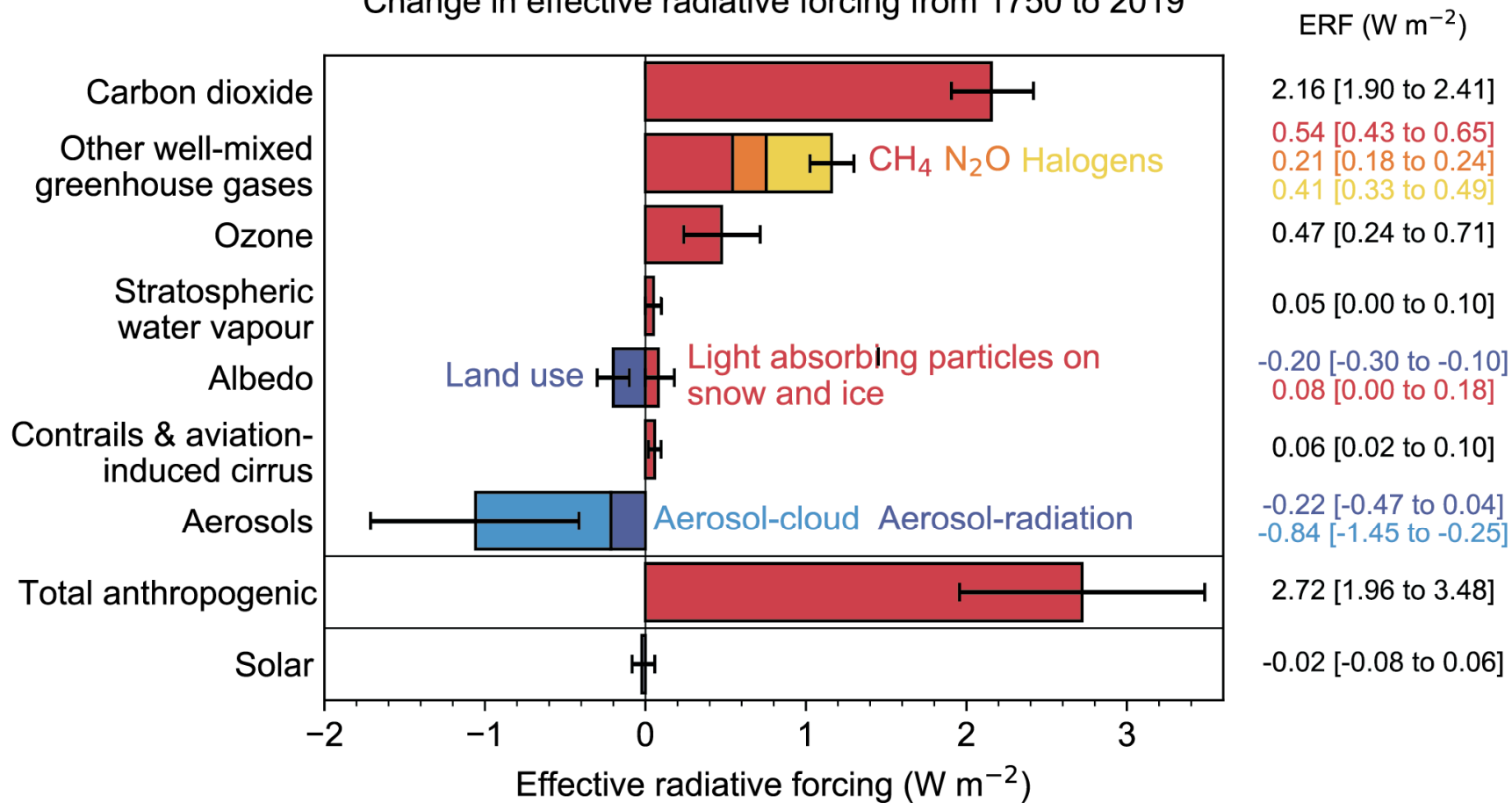
**Figure 7.8 | Attributed global surface air temperature change (GSAT) from 1750 to 2019 produced using the two-layer emulator (Supplementary Material 7.SM.2), forced with ERF derived in this chapter (displayed in Figure 2.10) and climate response constrained to assessed ranges for key climate metrics described in Cross-Chapter Box 7.1.** The results shown are the medians from a 2237-member ensemble that encompasses uncertainty in forcing and climate response (year-2019 best estimates and uncertainties are shown in Figure 7.7 for several components). Temperature contributions are expressed for carbon dioxide (CO<sub>2</sub>), methane (CH<sub>4</sub>), nitrous oxide (N<sub>2</sub>O), other well-mixed greenhouse gases (WMGHGs), ozone (O<sub>3</sub>), aerosols, and other anthropogenic forcings, as well as total anthropogenic, solar, volcanic, and total forcing. Shaded uncertainty bands show *very likely* (5–95%) ranges. Further details on data sources and processing are available in the chapter data table (Table 7.SM.14).



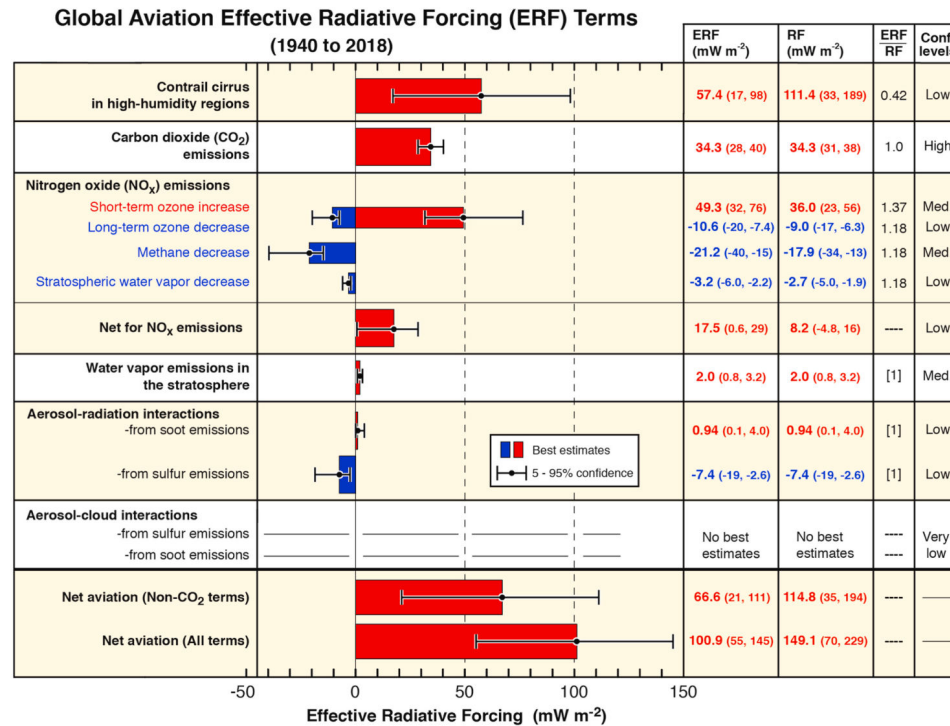
# Attributed global surface air temperature change (GSAT) from 1750 to 2019



### Change in effective radiative forcing from 1750 to 2019



# Effective radiative forcing (ERF) from aviation



Lee et al., 2021

$$\Delta T = \lambda \text{ ERF}$$

- The non-CO<sub>2</sub> effects contribute at least 2/3 to the total aviation ERF.
- The magnitude of the non-CO<sub>2</sub> effects depends on location and time of the emissions.



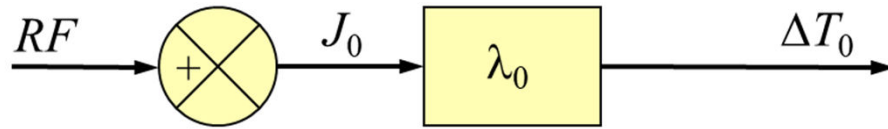
## Statements in the Executive Summary

### *Climate Feedbacks and Sensitivity (1)*

The net effect of changes in clouds in response to global warming is to amplify human-induced warming, that is, the net cloud feedback is positive (*high confidence*). Compared to AR5, major advances in the understanding of cloud processes have increased the level of confidence and decreased the uncertainty range in the cloud feedback by about 50%. An assessment of the low-altitude cloud feedback over the subtropical oceans, which was previously the major source of uncertainty in the net cloud feedback, is improved owing to a combined use of climate model simulations, satellite observations, and explicit simulations of clouds, altogether leading to strong evidence that this type of cloud amplifies global warming. The net cloud feedback, obtained by summing the cloud feedbacks assessed for individual regimes, is  $0.42 [-0.10 \text{ to } +0.94] \text{ W m}^{-2} \text{ } ^\circ\text{C}^{-1}$ . A net negative cloud feedback is *very unlikely (high confidence)*. {7.4.2, Figure 7.10, Table 7.10}



## Forcing, Response and Feedback

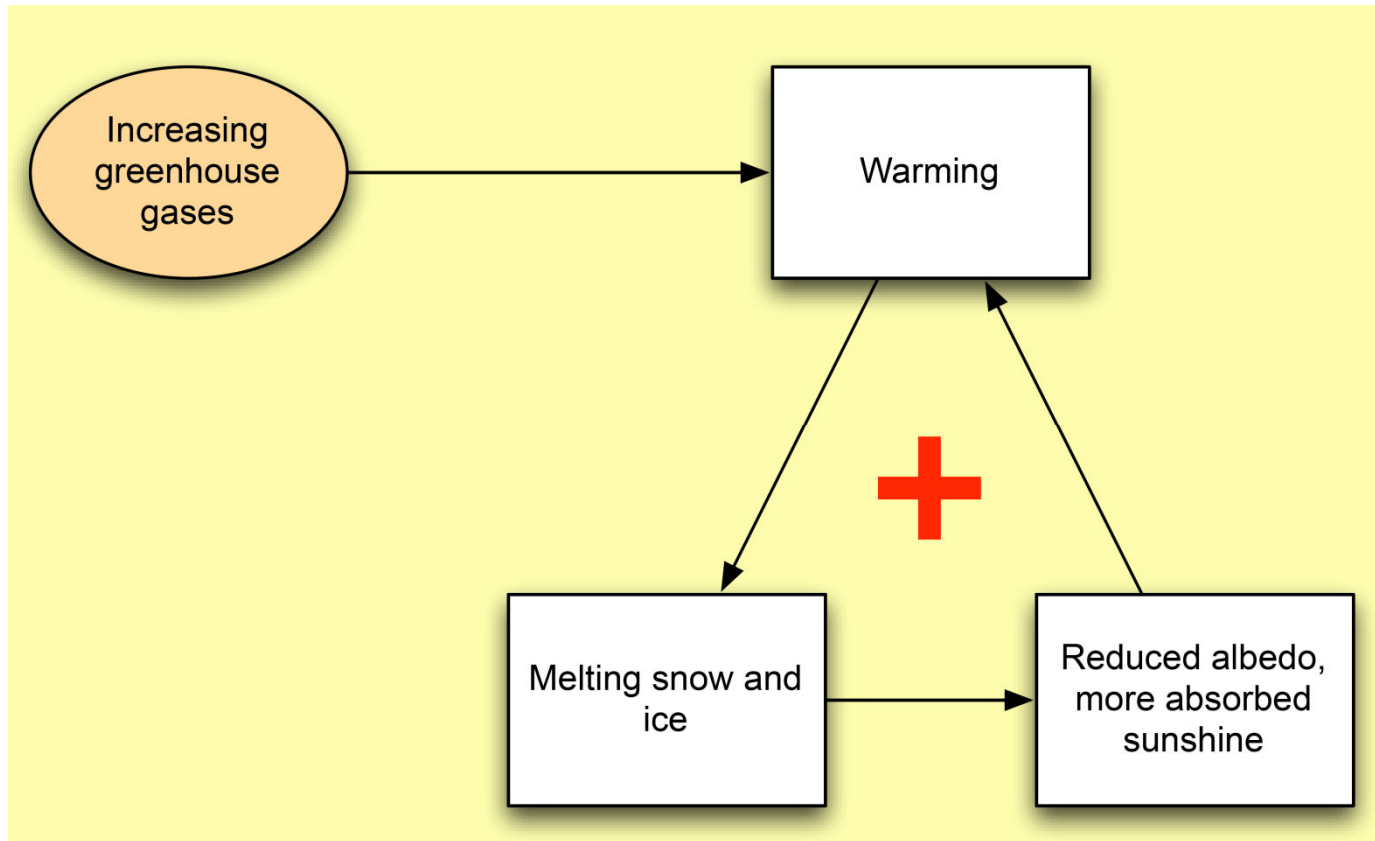


$$\Delta T_0 = \lambda_0 \cdot J_0 = \lambda_0 \cdot RF$$





## Example: Albedo feedback

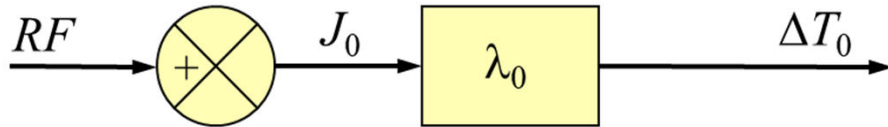


Randel, CSU, 2007



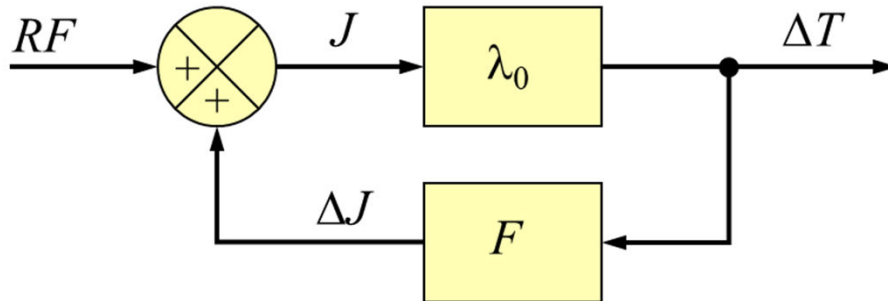
## Forcing, Response and Feedback

Geben Sie hier eine Formel ein.



$$\Delta T_0 = \lambda_0 \cdot J_0 = \lambda_0 \cdot RF$$

$$J = RF + \Delta J = RF + F \cdot \Delta T$$



$$\Delta T = \lambda_0 \cdot J = \lambda_0 \cdot (RF + F \cdot \Delta T) = \lambda \cdot RF$$

$$\frac{RF}{\Delta T} = \frac{1}{\lambda} = -\alpha$$

$$\alpha \approx \sum_i \alpha_i$$

climate sensitivity parameter:  $\lambda$

ratio of responses:  $r = \Delta T / \Delta T_0 = \lambda_0 / \lambda = 1 / (1 - f)$

feedback factor:  $f = F \cdot \lambda_0$

feedback:  $F$

feedback parameter:  $\alpha$



## Statements in the Executive Summary

### *Climate Feedbacks and Sensitivity (2)*

The combined effect of all known radiative feedbacks (physical, biogeophysical, and non-CO<sub>2</sub> biogeochemical) is to amplify the base climate response, also known as the Planck temperature response (*virtually certain*). Combining these feedbacks with the base climate response, the net feedback parameter based on process understanding is assessed to be  $-1.16$  [ $-1.81$  to  $-0.51$ ]  $\text{W m}^{-2} \text{ } ^\circ\text{C}^{-1}$ , which is slightly less negative than that inferred from the overall ECS assessment. The combined water-vapour and lapse-rate feedback makes the largest single contribution to global warming, whereas the cloud feedback remains the largest contribution to overall uncertainty. Due to the state-dependence of feedbacks, as evidenced from paleoclimate observations and from models, the net feedback parameter will increase (become less negative) as global temperature increases. Furthermore, on long time scales the ice-sheet feedback parameter is *very likely positive*, promoting additional warming on millennial time scales as ice sheets come into equilibrium with the forcing (*high confidence*).  
{7.4.2, 7.4.3, 7.5.7}



## Statements in the Executive Summary

### *Climate Feedbacks and Sensitivity (3)*

Radiative feedbacks, particularly from clouds, are expected to become less negative (more amplifying) on multi-decadal time scales as the spatial pattern of surface warming evolves, leading to an ECS that is higher than was inferred in AR5 based on warming over the instrumental record. This new understanding, along with updated estimates of historical temperature change, ERF, and Earth's energy imbalance, reconciles previously disparate ECS estimates (*high confidence*). However, there is currently insufficient evidence to quantify a *likely* range of the magnitude of future changes to current climate feedbacks. Warming over the instrumental record provides robust constraints on the lower end of the ECS range (*high confidence*), but owing to the possibility of future feedback changes it does not, on its own, constrain the upper end of the range, in contrast to what was reported in AR5. {7.4.4, 7.5.2, 7.5.3}



## Statements in the Executive Summary

### *Climate Feedbacks and Sensitivity (4)*

**Based on multiple lines of evidence the best estimate of ECS is 3 °C, the *likely* range is 2.5 °C to 4 °C, and the *very likely* range is 2 °C to 5 °C. It is virtually certain that ECS is larger than 1.5 °C.** Substantial advances since AR5 have been made in quantifying ECS based on feedback process understanding, the instrumental record, paleoclimates and emergent constraints. There is a high level of agreement among the different lines of evidence. All lines of evidence help rule out ECS values below 1.5 °C, but currently it is not possible to rule out ECS values above 5 °C. Therefore, the 5 °C upper end of the *very likely* range is assessed to have medium confidence and the other bounds have *high confidence*. {7.5.5}

**Based on process understanding, warming over the instrumental record, and emergent constraints, the best estimate of TCR is 1.8 °C, the *likely* range is 1.4 °C to 2.2 °C and the *very likely* range is 1.2 °C to 2.4 °C (*high confidence*). {7.5.5}**



## Statements in the Executive Summary

### *Climate Feedbacks and Sensitivity (5)*

On average, Coupled Model Intercomparison Project Phase 6 (CMIP6) models have higher mean ECS and TCR values than the Phase 5 (CMIP5) generation of models. They also have higher mean values and wider spreads than the assessed best estimates and **very likely ranges within this Report**. These higher ECS and TCR values can, in some models, be traced to changes in extra-tropical cloud feedbacks that have emerged from efforts to reduce biases in these clouds compared to satellite observations (*medium confidence*). The broader ECS and TCR ranges from CMIP6 also lead the models to project a range of future warming that is wider than the assessed warming range, which is based on multiple lines of evidence. However, some of the high-sensitivity CMIP6 models are less consistent with observed recent changes in global warming and with paleoclimate proxy data than models with ECS within the *very likely* range. Similarly, some of the low-sensitivity models are less consistent with the paleoclimate data. The CMIP models with the highest ECS and TCR values provide insights into low-likelihood, high-impact outcomes, which cannot be excluded based on currently available evidence (*high confidence*). {4.3.1, 4.3.4, 7.4.2, 7.5.6}



# Global mean climate feedbacks

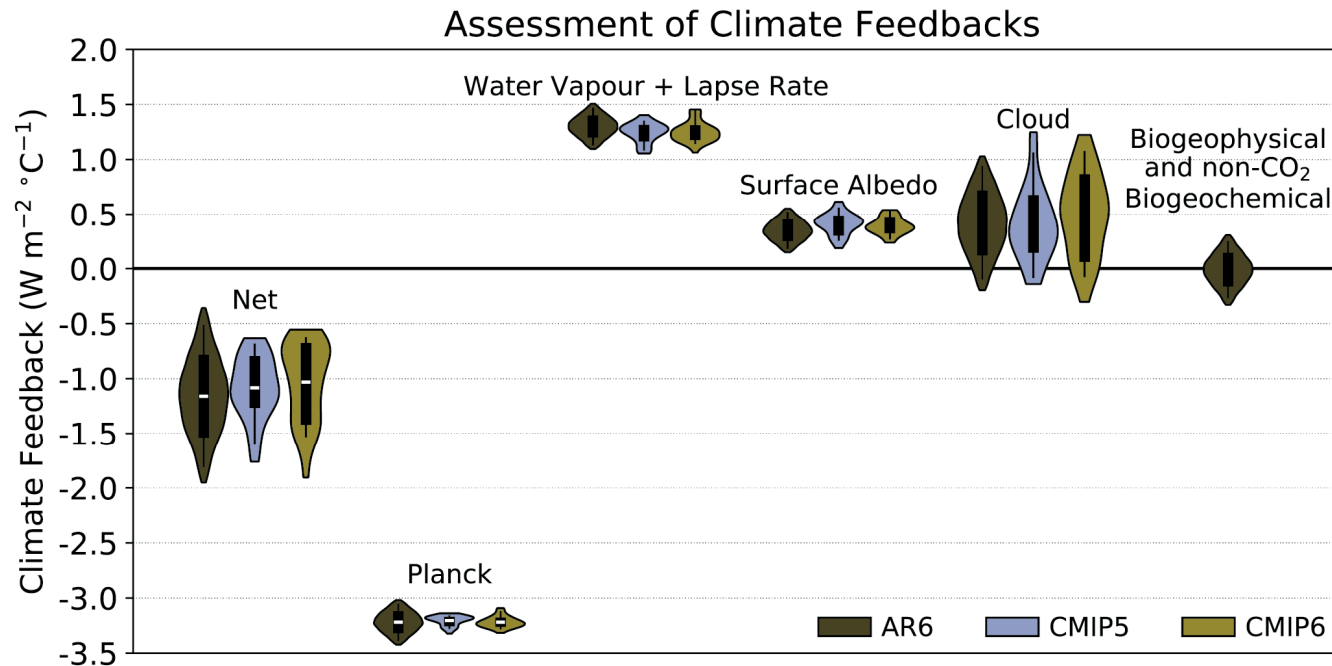


**Figure 7.10 | Global mean climate feedbacks estimated in *abrupt4xCO2* simulations of 29 CMIP5 models (light blue) and 49 CMIP6 models (orange), compared with those assessed in this Report (red).** Individual feedbacks for CMIP models are averaged across six radiative kernels as computed in Zelinka et al. (2020). The white line, black box and vertical line indicate the mean, 66% and 90% ranges, respectively. The shading represents the probability distribution across the full range of GCM/ESM values and for the 2.5–97.5 percentile range of the AR6 normal distribution. The unit is  $W m^{-2} °C^{-1}$ . Feedbacks associated with biogeophysical and non-CO<sub>2</sub> biogeochemical processes are assessed in AR6, but they are not explicitly estimated from general circulation models (GCMs)/Earth system models (ESMs) in CMIP5 and CMIP6. Further details on data sources and processing are available in the chapter data table (Table 7.SM.14).

## Statements in the Executive Summary

### *Climate Response (1)*

The total human-forced GSAT change from 1750 to 2019 is calculated to be 1.29 [0.99 to 1.65] °C. This calculation is an emulator-based estimate, constrained by the historic GSAT and ocean heat content changes from Chapter 2 and the ERF, ECS and TCR from this chapter. The calculated GSAT change is composed of a well-mixed greenhouse gas warming of 1.58 [1.17 to 2.17] °C (*high confidence*), a warming from ozone changes of 0.23 [0.11 to 0.39] °C (*high confidence*), a cooling of  $-0.50$  [ $-0.22$  to  $-0.96$ ] °C from aerosol effects (*medium confidence*), and a  $-0.06$  [ $-0.15$  to  $+0.01$ ] °C contribution from surface reflectance changes from land-use change and light-absorbing particles on ice and snow (*medium confidence*). Changes in solar and volcanic activity are assessed to have together contributed a small change of  $-0.02$  [ $-0.06$  to  $+0.02$ ] °C since 1750 (*medium confidence*). {7.3.5}





## ECS and TCR

**ECS**    **equilibrium climate sensitivity**

equilibrium temperature change after CO<sub>2</sub> doubling

**TCR**    **transient climate response**

temperature change in transient simulation with an annual CO<sub>2</sub> increase of 1% at the time when a CO<sub>2</sub> doubling is achieved



# ERF due to CO<sub>2</sub> increase and temperature response

Process assessment of Transient Climate Response

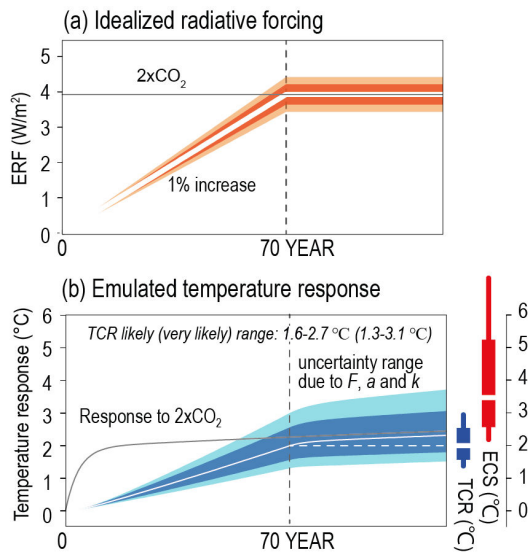
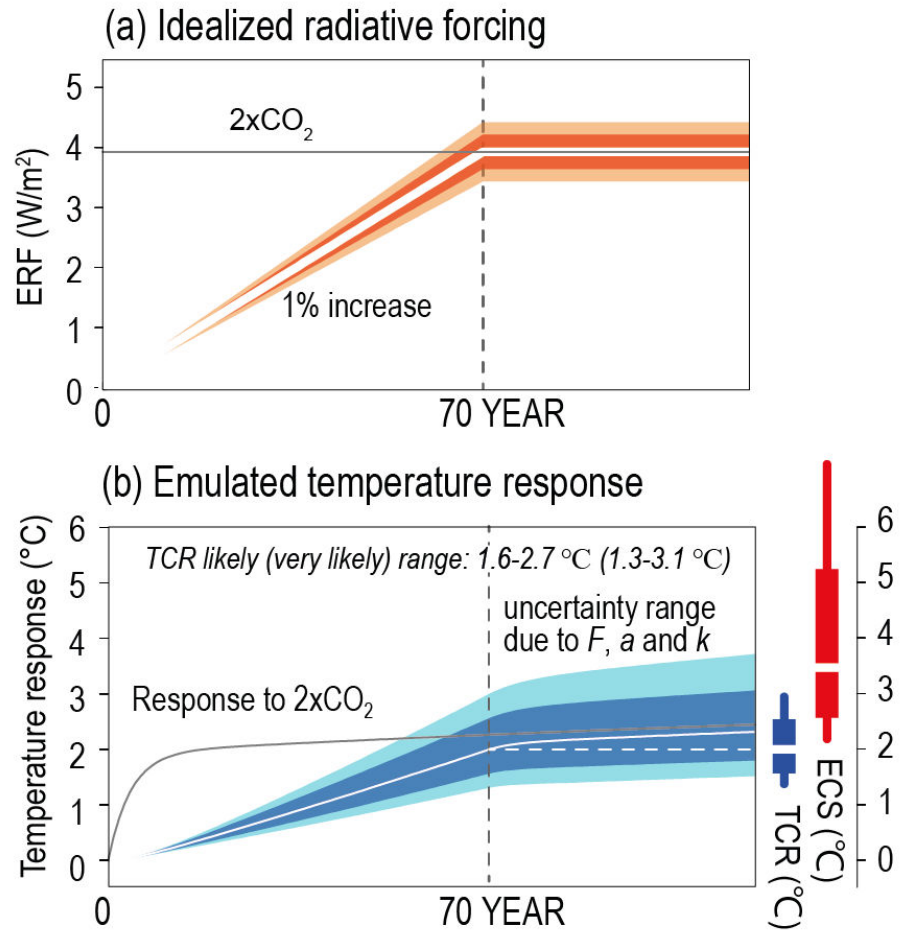


**Figure 7.17 | (a) Time evolution of the effective radiative forcing (ERF) to the CO<sub>2</sub> concentration increased by 1% per year until year 70 (equal to the time of doubling) and kept fixed afterwards (white line).** The *likely* and *very likely* ranges of ERF indicated by light and dark orange have been assessed in Section 7.3.2.1. **(b) Surface temperature response to the CO<sub>2</sub> forcing calculated using the emulator with a given value of ECS, considering uncertainty in  $\Delta F_{2\times CO_2}$ ,  $\alpha$ , and  $\kappa$  associated with the ocean heat uptake and efficacy (white line).** The *likely* and *very likely* ranges are indicated by cyan and blue, respectively. For comparison, the temperature response to abrupt doubling of the CO<sub>2</sub> concentration is displayed by a grey curve. The mean, *likely* and *very likely* ranges of ECS and TCR are shown at the right (the values of TCR also presented in the panel). Further details on data sources and processing are available in the chapter data table (Table 7.SM.14).

# Process assessment of Transient Climate Response



IPCC 2013, Chap. 7

## Statements in the Executive Summary

### *Climate Response (2)*

**Uncertainties regarding the true value of ECS and TCR are the dominant source of uncertainty in global temperature projections over the 21st century under moderate to high greenhouse gas emissions scenarios. For scenarios that reach net zero carbon dioxide emissions, the uncertainty in the ERF values of aerosol and other short-lived climate forcers contribute substantial uncertainty in projected temperature. Global ocean heat uptake is a smaller source of uncertainty in centennial-time scale surface warming (*high confidence*). {7.5.7}**



# ECS and TCR assessments using different lines of evidence

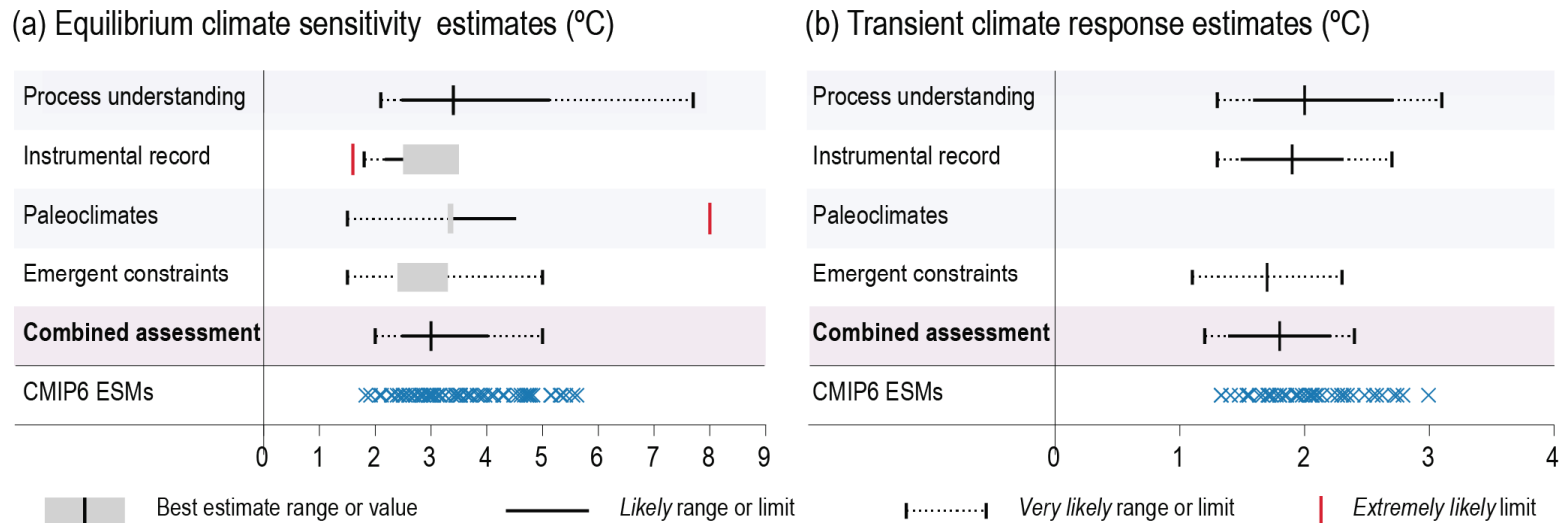
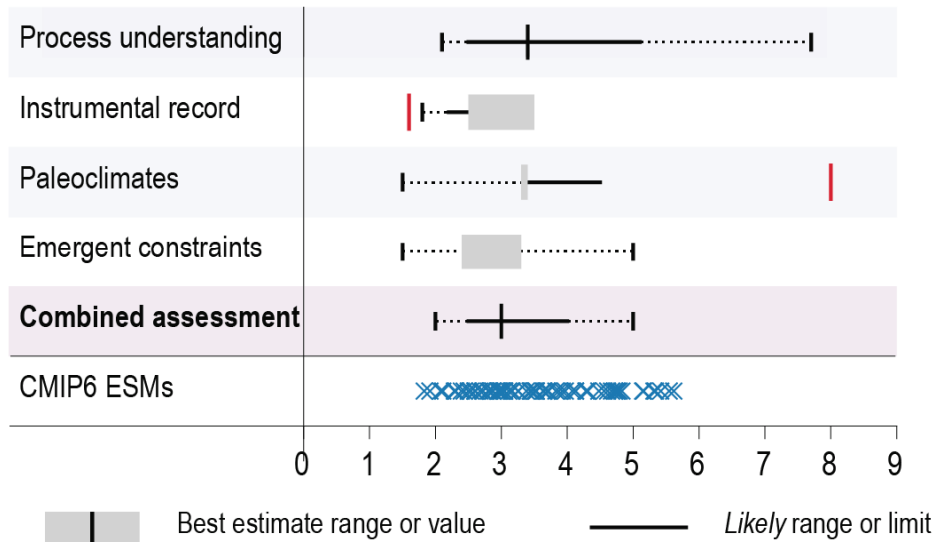


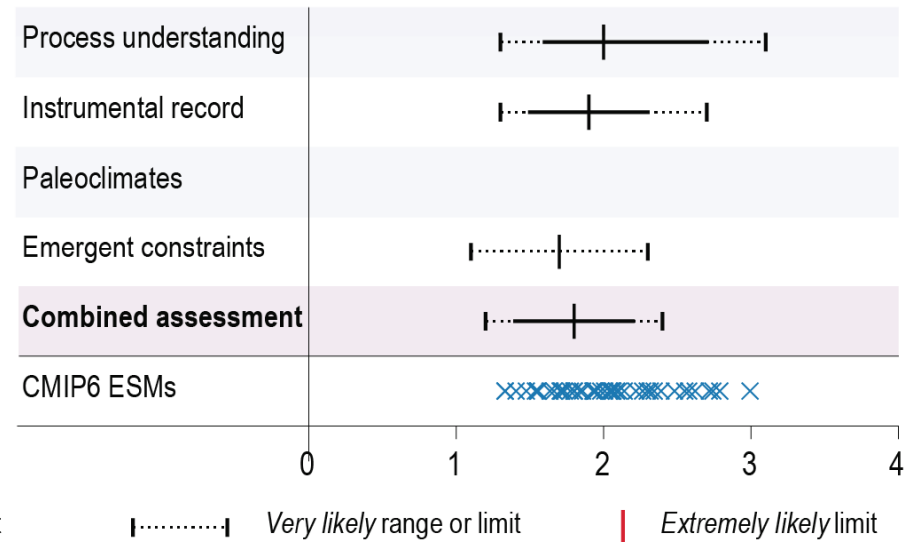
**Figure 7.18 | Summary of the equilibrium climate sensitivity (ECS panel (a)) and transient climate response (TCR panel (b)) assessments using different lines of evidence.** Assessed ranges are taken from Tables 7.13 and 7.14 for ECS and TCR respectively. Note that for the ECS assessment based on both the instrumental record and paleoclimates, limits (i.e., one-sided distributions) are given, which have twice the probability of being outside the maximum/minimum value at a given end, compared to ranges (i.e., two-tailed distributions) which are given for the other lines of evidence. For example, the *extremely likely* limit of greater than 95% probability corresponds to one side of the *very likely* (5–95%) range. Best estimates are given as either a single number or by a range represented by a grey box. CMIP6 model values are not directly used as a line of evidence but presented on the Figure for comparison. ECS values are taken from Schlund et al. (2020) and TCR values from Meehl et al. (2020); see Supplementary Material 7.SM.4. Further details on data sources and processing are available in the chapter data table (Table 7.SM.14).

# ECS and TCR assessments using different lines of evidence

(a) Equilibrium climate sensitivity estimates (°C)



(b) Transient climate response estimates (°C)



## Statements in the Executive Summary

### *Climate Response (3)*

**The assessed historical and future ranges of GSAT change in this Report are shown to be internally consistent with the Report's assessment of key physical-climate indicators: greenhouse gas ERFs, ECS and TCR.** When calibrated to match the assessed ranges within the assessment, physically based emulators can reproduce the best estimate of GSAT change over 1850–1900 to 1995–2014 to within 5% and the *very likely* range of this GSAT change to within 10%. Two physically based emulators match at least two-thirds of the Chapter 4-assessed projected GSAT changes to within these levels of precision. When used for multi-scenario experiments, calibrated physically based emulators can adequately reflect assessments regarding future GSAT from Earth system models and/or other lines of evidence (*high confidence*). {Cross-Chapter Box 7.1}



## Statements in the Executive Summary

### *Climate Response (4)*

It is now well understood that the Arctic warms more quickly than the Antarctic due to differences in radiative feedbacks and ocean heat uptake between the poles, but that surface warming will eventually be amplified in both the Arctic and Antarctic (*high confidence*). The causes of this polar amplification are well understood, and the evidence is stronger than at the time of AR5, supported by better agreement between modelled and observed polar amplification during warm paleo time periods (*high confidence*). The Antarctic warms more slowly than the Arctic owing primarily to upwelling in the Southern Ocean, and even at equilibrium is expected to warm less than the Arctic. The rate of Arctic surface warming will continue to exceed the global average over this century (*high confidence*). There is also *high confidence* that Antarctic amplification will emerge as the Southern Ocean surface warms on centennial time scales, although only *low confidence* regarding whether this feature will emerge during the 21st century. {7.4.4}





## Statements in the Executive Summary

### *Climate Response (5)*

The assessed global warming potentials (GWP) and global temperature-change potentials (GTP) for methane and nitrous oxide are slightly lower than in AR5 due to revised estimates of their lifetimes and updated estimates of their indirect chemical effects (*medium confidence*). The assessed metrics now also include the carbon cycle response for non-CO<sub>2</sub> gases. The carbon cycle estimate is lower than in AR5, but there is *high confidence* in the need for its inclusion and in the quantification methodology. Metrics for methane from fossil fuel sources account for the extra fossil CO<sub>2</sub> that these emissions contribute to the atmosphere and so have slightly higher emissions metric values than those from biogenic sources (*high confidence*). {7.6.1}



## Emission metrics (1)

**GWP Global Warming Potential**

$$AGWP_i^H = \int_0^H RF_i(t) dt$$
$$GWP_i = \frac{AGWP_i}{AGWP_{CO_2}}$$

**GTP Global Temperature change Potential**

$$GTP_i^H = \frac{\Delta T_i^H}{\Delta T_{CO_2}^H}$$

$H$  time horizon



## Statements in the Executive Summary

### *Climate Response (6)*

**New emissions metric approaches such as GWP\* and the combined-GTP (CGTP) are designed to relate emissions rates of short-lived gases to cumulative emissions of CO<sub>2</sub>. These metric approaches are well suited to estimate the GSAT response from aggregated emissions of a range of gases over time, which can be done by scaling the cumulative CO<sub>2</sub> equivalent emissions calculated with these metrics by the transient climate response to cumulative emissions of CO<sub>2</sub>. For a given multi-gas emissions pathway, the estimated contribution of emissions to surface warming is improved by using either these new metric approaches or by treating short- and long-lived GHG emissions pathways separately, as compared to approaches that aggregate emissions of GHGs using standard GWP or GTP emissions metrics. By contrast, if emissions are weighted by their 100-year GWP or GTP values, different multi-gas emissions pathways with the same aggregated CO<sub>2</sub> equivalent emissions rarely lead to the same estimated temperature outcome (*high confidence*). {7.6.1, Box 7.3}**



## Emission metrics (2)

**ATR** Average Temperature Response

$$ATR_i^H = \frac{1}{H} \int_0^H \Delta T_i(t) dt$$
$$\frac{ATR_i^H}{ATR_{CO_2}^H}$$

**GWP\*** Global Temperature change Potential

$$GWP_i^{*H} \approx \frac{\Delta e_i^h}{h} H GWP_i^H$$

$\Delta e_i^h$

change of emissions during previous time period  $h$



## Statements in the Executive Summary

### *Climate Response (7)*

**The choice of emissions metric affects the quantification of net zero GHG emissions and therefore the resulting temperature outcome after net zero emissions are achieved.** In general, achieving net zero CO<sub>2</sub> emissions and declining non-CO<sub>2</sub> radiative forcing would be sufficient to prevent additional human-caused warming. Reaching net zero GHG emissions as quantified by GWP-100 typically results in global temperatures that peak and then decline after net zero GHGs emissions are achieved, though this outcome depends on the relative sequencing of mitigation of short-lived and long-lived species. In contrast, reaching net zero GHG emissions when quantified using new emissions metrics such as CGTP or GWP\* would lead to approximate temperature stabilization (*high confidence*). {7.6.2}

